Final Report

OCULAR LASER THRESHOLD INVESTIGATIONS

By: ARTHUR VASSILIADIS H. C. ZWENG .. G. DEDRICK

Prepared for:

UNITED STATES AIR FORCE
SCHOOL OF AEROSPACE MEDICINE
AEROSPACE MEDICAL DIVISION (AFSC)
BROOKS AIR FORCE BASE, TEXAS

CONTRACT F41609-70-C-0002

STANFORD RESEARCH INSTITUTE
Menlo Park, California 94025 · U.S.A.

63

UNCLASSIFIED

Security Classification

DOCUMENT CONTROL DATA - R & D

(Security classification of title, body of abstract and indexing annotation must be entered when the overall report is classified)

1. ORIGINATING ACTIVITY *(Corporate author)*
Stanford Research Institute
333 Ravenswood Avenue
Menlo Park, California 94025

2a. REPORT SECURITY CLASSIFICATION
UNCLASSIFIED

2b. GROUP
N/A

3. REPORT TITLE

OCULAR LASER THRESHOLD INVESTIGATIONS

4. DESCRIPTIVE NOTES *(Type of report and inclusive dates)*
Final Report Covering the period 1 September 1969 to 31 December 1970

5. AUTHOR(S) *(First name, middle initial, last name)*

Arthur Vassiliadis H. Christian Zweng Kent G. Dedrick

6. REPORT DATE	7a. TOTAL NO OF PAGES	7b. NO OF REFS
January 1971	62	13

8a. CONTRACT OR GRANT NO.	9a. ORIGINATOR'S REPORT NUMBER(S)
Contract F41609-70-C-0002	Final Report
b. PROJECT NO.	SRI Project 8209
c.	9b. OTHER REPORT NO(S) *(Any other numbers that may be assigned this report)*
d.	

10. DISTRIBUTION STATEMENT

Approved for public release; distribution unlimited.

11. SUPPLEMENTARY NOTES

Details of illustrations in this document may be better studied on microfiche

12. SPONSORING MILITARY ACTIVITY
United States Air Force
School of Aerospace Medicine
Aerospace Medical Division (AFSC)
Brooks Air Force Base, Texas

13. ABSTRACT

Results of experimental investigations to determine threshold levels for doubled neodymium and ruby lasers are presented. The experimental animals were rhesus monkeys.

Threshold levels for retinal damage caused by the doubled long-pulsed and Q-switched neodymium laser are reported, and results of experiments to determine retinal damage and lens damage caused by the Q-switched ruby laser are presented.

In addition, theoretical considerations and calculations for retinal damage are discussed and compared with experimental results.

DD FORM 1 NOV 68 1473 (PAGE 1)

S/N 0101-807-6801

UNCLASSIFIED

Security Classification

14 KEY WORDS	LINK A		LINK B		LINK C	
	ROLE	WT	ROLE	WT	ROLE	WT
Lasers						
Retinal damage						
Lens damage						
Ophthalmology						
Thermal models						

OCULAR LASER THRESHOLD INVESTIGATIONS

By: ARTHUR VASSILIADIS H. C. ZWENG K. G. DEDRICK

Prepared for:

UNITED STATES AIR FORCE
SCHOOL OF AEROSPACE MEDICINE
AEROSPACE MEDICAL DIVISION (AFSC)
BROOKS AIR FORCE BASE, TEXAS

CONTRACT F41609-70-C-0002

SRI Project 8209

Approved by:

CHARLES J. SHOENS, *Director*
Electromagnetic Techniques Laboratory

RAY L. LEADABRAND, *Executive Director*
Electronics and Radio Sciences Division

Copy No. 33

ABSTRACT

Results of experimental investigations to determine threshold levels for doubled neodymium and ruby lasers are presented. The experimental animals were rhesus monkeys.

Threshold levels for retinal damage caused by the doubled long-pulsed and Q-switched neodymium laser are reported, and results of experiments to determine retinal damage and lens damage caused by the Q-switched ruby laser are presented.

In addition, theoretical considerations and calculations for retinal damage are discussed and compared with experimental results.

FOREWORD

The research program discussed in this Final Report was conducted under Contract F41609-70-C-0002, Project 6301, Task 630105, supported by the USAF School of Aerospace Medicine, Aerospace Medical Division, Brooks Air Force Base, Texas. The project monitor was Maj. I. Dunsky.

The research reported covers the period 1 September 1969 to 31 December 1970. The project leader, Dr. A. Vassiliadis, was responsible for the research activity under SRI Project 8209.

The experiments reported herein were conducted according to the "Principles of Laboratory Animal Care," established by the National Society of Medical Research.

Publication of this report does not constitute Air Force approval of the report's findings or conclusions. It is published only for the exchange and stimulation of ideas.

CONTENTS

ABSTRACT ii

FOREWORD iii

LIST OF ILLUSTRATIONS vi

I INTRODUCTION 1

II EXPERIMENTAL DAMAGE THRESHOLDS 3

A. General Remarks 3

B. Doubled Q-Switched Neodymium 5

1. Laser Characteristics 5
2. Experiments and Results 6

C. Doubled Long-Pulsed Neodymium 7

1. Laser Characteristics 7
2. Experiments and Results 11

D. Doubled Q-Switched Ruby 11

1. Laser Characteristics 11
2. Retinal Experiments and Results 14
3. Lens-Damage Experiments and Results 15

III THEORETICAL CONSIDERATIONS OF RETINAL DAMAGE 24

A. Absorption of Light in the Fundus 24

B. Thermal Damage 25

C. Models for Retinal Damage 25

D. Temperature Variation in Retinal Exposures 26

E. Thermal Rate Processes 28

F. Comparison of Theory and Experimental Results . . . 35

IV CONCLUSIONS 44

ACKNOWLEDGMENTS 45

Appendix--HEAT-FLOW PROBLEM 46

REFERENCES. 51

DD Form 1473

ILLUSTRATIONS

Figure 1(a)	Photograph of the Delivery System.	4
Figure 1(b)	Diagram of the Delivery System	4
Figure 2	Typical Pulse of Doubled Q-Switched Neodymium Laser.	6
Figure 3	Paramacular Damage to Rhesus Monkey Retina with Doubled Q-Switched Neodymium.	8
Figure 4	Macular Damage to Rhesus Monkey Retina with Doubled Q-Switched Neodymium	9
Figure 5	Typical Pulse Train of Long-Pulsed Neodymium Laser.	10
Figure 6	Paramacular Damage to Rhesus Monkey Retina with Doubled Long-Pulsed Neodymium	12
Figure 7	Macular Damage to Rhesus Monkey Retina with Doubled Long-Pulsed Neodymium	13
Figure 8	Typical Output Pulse of Q-Switched Ruby Laser.	14
Figure 9	Summary of Retinal Exposures of Rhesus Monkeys to Doubled Q-Switched Ruby	16
Figure 10	Small Lens Opacities in Rhesus Monkey One Month After Exposure to Doubled Q-Switched Ruby.	17
Figure 11	Rhesus Monkey Lens Opacities One Month After Exposure to Doubled Q-Switched Ruby. . .	18
Figure 12	Rhesus Monkey Lens Opacity Three Months After Exposure to Doubled Q-Switched Ruby. . .	19

Figure 13	Posterior Surface Lens Change in Rhesus Monkey After Doubled Ruby Laser Exposure . . .	20
Figure 14	Rhesus Monkey Lenticular Damage Based on Immediate Post-Operative Observation for Exposure to Doubled Q-Switched Ruby.	21
Figure 15	Rhesus Monkey Lenticular Damage Based on Three-Month Post-Operative Observation for Exposure to Doubled Q-Switched Ruby.	22
Figure 16	Temperature Rise as a Function of Time for Various Spot Sizes at the Center of the Absorbing Disc--Uniform Beam Cross Section . .	29
Figure 17	Temperature Rise as a Function of Time for Various Distances from Center of a Disc--Uniform Beam Cross Section	30
Figure 18	Temperature Rise as a Function of Time for Various Spot Sizes at Center of Absorbing Disc--Gaussian Beam Cross Section. .	31
Figure 19	Temperature Rise as a Function of Time for Various Distances from Center of Disc--Gaussian Beam Cross Section.	32
Figure 20	Threshold Retinal Damage in Rhesus Monkey for Argon Laser.	36
Figure 21	Comparison of Relative Shape of Threshold Variation for Simple Model with Actual Data--Assuming Only Pigment Epithelium Layer Absorbing.	37
Figure 22	Comparison of Relative Shape of Threshold Variation for Two Thicknesses of the Pigment Epithelium Layer for Various Retinal Spot Sizes	38
Figure 23	Relative Threshold Variations for Three Inactivation Energies.	40

Figure 24 Comparison of Relative Shape of Threshold Variation for Inactivation Thermal Model with Experimental Data 40

Figure 25 Comparison of Simple Models--Relative Shape of Threshold Variation as a Function of Spot Size 42

ADDENDUM

The following information is presented for the convenience of the reader, to clarify certain aspects of the Final Report on SRI Project 8209, "Ocular Laser Threshold Investigations," dated January 1971:

(1) The drugs used to tranquilize and anesthetize the rhesus monkeys were the following:

- Sernylan - Phencyclidine Hydrochloride - Parke Davis Co., Detroit, Michigan.

  Dose - 0.04 cc/kg.

- Diabutal - Sodium Pentobarbital - Diamond Labs., Des Moines, Iowa.

  Dose - 0.2 cc/kg.

(2) The focal lengths of lenses used to reduce the beam diameter in the doubled Q-switched neodymium laser were approximately 6 cm for the positive lens and 3 cm for the negative lens.

(3) The focal lengths of lenses used in the doubled long-pulsed neodymium laser were approximately 6 cm for the positive lens and 1.7 cm for the negative lens.

(4) The value for the lens used to correct for the refractive error at doubled ruby wavelength was calculated from refractive-index variation, as a function of wavelength, estimated for the ocular media.

(5) When a monkey had an eye with excessive astigmatism it was not used in retinal experiments. Thus, all monkeys used in retinal experiments had exposures in both eyes.

(6) The titles of References 8, 9, and 10 were omitted in the Final Report and are provided in the following:

8. W. T. Ham et al., "Effects of Laser Radiation on the Mammalian Eye," Trans. N.Y. Acad. Sci., Vol. 28, p. 517 (1966).

9. A. M. Clarke et al., "An Equilibrium Thermal Model for Retinal Injury from Optical Sources," Appl. Optics, Vol. 8, p. 1051 (1969).

10. W. P. Hansen et al., "A Worst-Case Analysis of Continuous Wave He-Ne Laser Hazards to the Eye," Appl. Optics, Vol. 6, p. 1973 (1967).

I INTRODUCTION

Over the past few years, concern for the hazards associated with exposure to bright sources of optical radiation has resulted in extensive studies by a number of investigators. In this work, particular emphasis has been given to the damage effects of a number of lasers in the visible and infrared parts of the spectrum.

This report summarizes damage data for some additional wavelengths and represents a continuation of work that has been carried out at Stanford Research Institute over the past five years. Although data for a number of the important lasers had been obtained,[1-3]* there were no studies to cover the doubled output of the two most commonly used lasers--i.e., ruby and neodymium doped materials. For this reason, the main emphasis of the research discussed in this report was on damage thresholds for doubled neodymium (530 nm) and doubled ruby (347 nm) wavelengths.

Threshold experiments for doubled neodymium were made for both long-pulsed and Q-switched modes of operation. Since the doubled wavelength is transmitted well by the ocular media, retinal damage is of major concern, and the threshold data were obtained for retinal damage.

In contrast, the doubled output of ruby, being in the ultraviolet, is absorbed by the ocular media. Thus, damage to the cornea, or lens becomes possible. Experiments were therefore carried out to study possible damage to the lens as well as to the retina.

---

*References are listed at the end of the report.

This report also includes a summary of some theoretical considerations that emerged in the course of the program. The principal calculations that are presented show, using a simple model for the retina and the choroid, how the temperature variations of laser exposures develop. The theoretical calculations are compared with experimental data, and inconsistencies are noted and discussed. It is also argued that rate processes in the damage mechanism must be considered in order to explain the temperature variations observed.

There is a brief discussion of the rate processes in thermal damage phenomena, and an approximate estimate of the inactivation energy of the proteins or enzymes involved in the threshold-damage type of interaction.

II EXPERIMENTAL DAMAGE THRESHOLDS

A. General Remarks

The exposures to the retina and to the lens were made at a special test station. This delivery system is built around a Zeiss fundus camera and has been described in previous reports.[2,3] A photograph of the delivery system in use is shown in Figure 1(a) and a diagram of the system is shown in Figure 1(b).

The delivery system provides a means of selecting a small part of the laser beam and accurately monitoring it and directing it into the eye. In order to select a relatively uniform part of the laser beam an adjustable iris was used, and the laser itself was located at the largest practical distance from the delivery point.

In each of the experiments the doubled laser was carefully aligned with the delivery system with the aid of a He-Ne laser. Calibration of the delivery system was made by placing a ballistic thermopile at the corneal plane of the animal's eye and measuring the energy at the thermopile and at the detector that was used for monitoring. This calibration was made near the laser so that the whole doubled output could be introduced into the thermopile, thus providing adequate energy to perform the calibration.

The rhesus monkeys used in the experiments were given atropine for at least three days prior to the day of the exposure. This provided adequate paralysis of accommodation in the rhesus eye so that the experiment could be performed with minimum changes in refractive error. In addition, this provided maximum dilation of the iris, which was required both for the retinal and the lens exposures.

FIGURE 1(a) PHOTOGRAPH OF THE DELIVERY SYSTEM

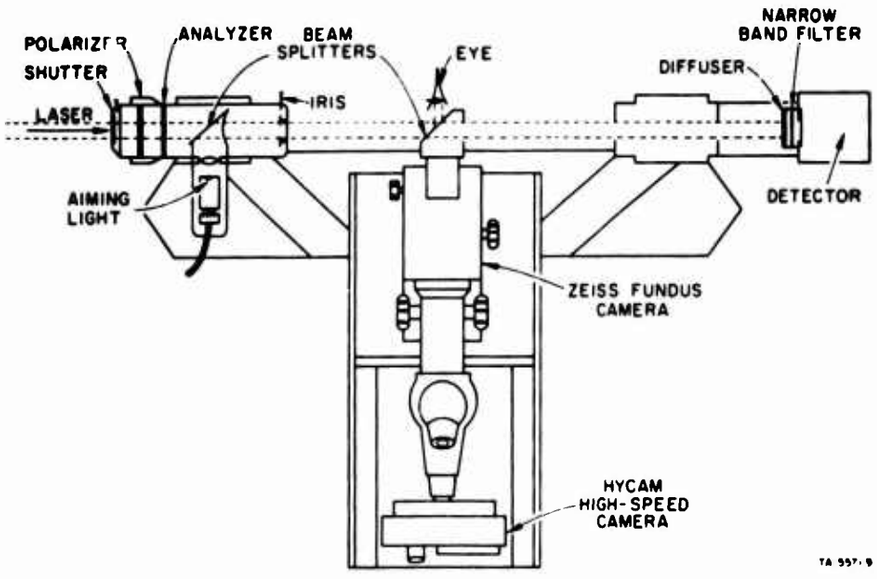

FIGURE 1(b) DIAGRAM OF THE DELIVERY SYSTEM

The day of the exposure, the animals were tranquilized with Sernylan and then put in deep anesthesia with sodium pentobarbital.[1] At least ten minutes were allowed to elapse from the time of deep anesthesia to the time the animal was refracted for the experiment. This assured that the changes in refraction that follow the drug administration had subsided. The refraction was made to the nearest 0.25 diopter and the appropriate lens was placed in front of the animal's eye during the experiment. If an animal had astigmatism of over 0.5 diopter it was not used in the retinal experiments.

B. Doubled Q-Switched Neodymium

1. Laser Characteristics

The neodymium laser cavity comprised a 6-inch rod 1/2 inch in diameter that has Brewster-angle cuts. The rod was water-cooled and pumped with two air-cooled linear flash lamps. The laser was Q-switched by a spinning quartz prism turning at 500 rps that was optimumly timed to switch the cavity Q. A sapphire flat Fabry-Perot served as the output end.

The output beam was reduced in diameter by a factor of two by the use of two lenses. The beam was then passed through an accurately oriented ADP crystal with which the 530-nm radiation was obtained. A photograph of a typical pulse is shown in Figure 2. The conversion efficiency in the doubler was not very good--typically 3 to 5 percent. However, this provided more than adequate energies at the test station, as described in the next section.

The doubled Q-switched laser was located approximately 35 feet from the delivery system. The divergence of the beam at the test station was measured to be 1.7 mrad. Thus, the spot size at the retina, although

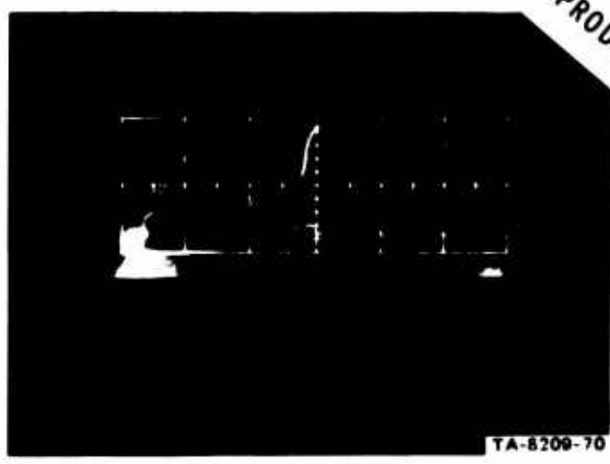

FIGURE 2 TYPICAL PULSE OF DOUBLED Q-SWITCHED NEODYMIUM LASER

determined by the animal's eye optics, will be greater than approximately 23 μ.

2. Experiments and Results

The experiments initially involved a large number of exposures in the paramacular area. In initial experiments, animals received 16 paramacular exposures and four macular exposures. The paramacular exposures were all placed within the temporal superior and inferior vessel arcades. Thus, the exposures were in the immediate neighborhood of the macula and near the posterior pole. Since the primary interest is in the macular threshold level, the large majority of the experiments were made with eight paramacular exposures and four macular exposures in each eye.

The procedure used was similar to the protocols of previous experiments.[1-3] Thus, the laser exposures were placed in the eye and the observation to determine whether a lesion has formed was made one hour after exposure. Each exposure site was examined and classified as either damaged or not damaged.

The retinal response for these exposures is similar to those observed in previous Q-switched experiments.[1,2] Thus, near threshold, no immediate response is seen. As the level is increased, however, a point is reached where an immediate response is seen. This has the appearance of a small white patch interpreted as edema, easily visible through an ophthalmoscope.

The experimental results presented in this section are a summary of the data on 20 rhesus monkeys. The data are presented separately as macular and paramacular. For each set of data the individual exposures are shown in a figure, and a probability curve is presented for each case.

The data for the paramacular area are summarized in Figure 3. From the data it is apparent that the low side of the damage level was stressed in order to assure that the threshold that is obtained is meaningful. The data show that the 50-percent probability for damage occurs at about 10 μJ. This may be compared with the Q-switched ruby data, which show a 50-percent damage probability at about 20 μJ.[1]

The macular data summarized in Figure 4 show a 50-percent probability for damage at about 5 μJ. This is appreciably lower than for the paramacular area. This same trend has been observed for Q-switched neodymium,[2] long-pulsed ruby,[1] and short He-Ne laser exposures.[4]

C. Doubled Long-Pulsed Neodymium

1. Laser Characteristics

The neodymium laser cavity used in this experiment was the same as that used in the Q-switched experiments. Instead of a spinning prism, however, a stationary homosil-quartz roof prism was used as the back end of the cavity. The laser was operated in a long-pulse mode with a typical pulse train lasting approximately 600 μs, as shown in Figure 5.

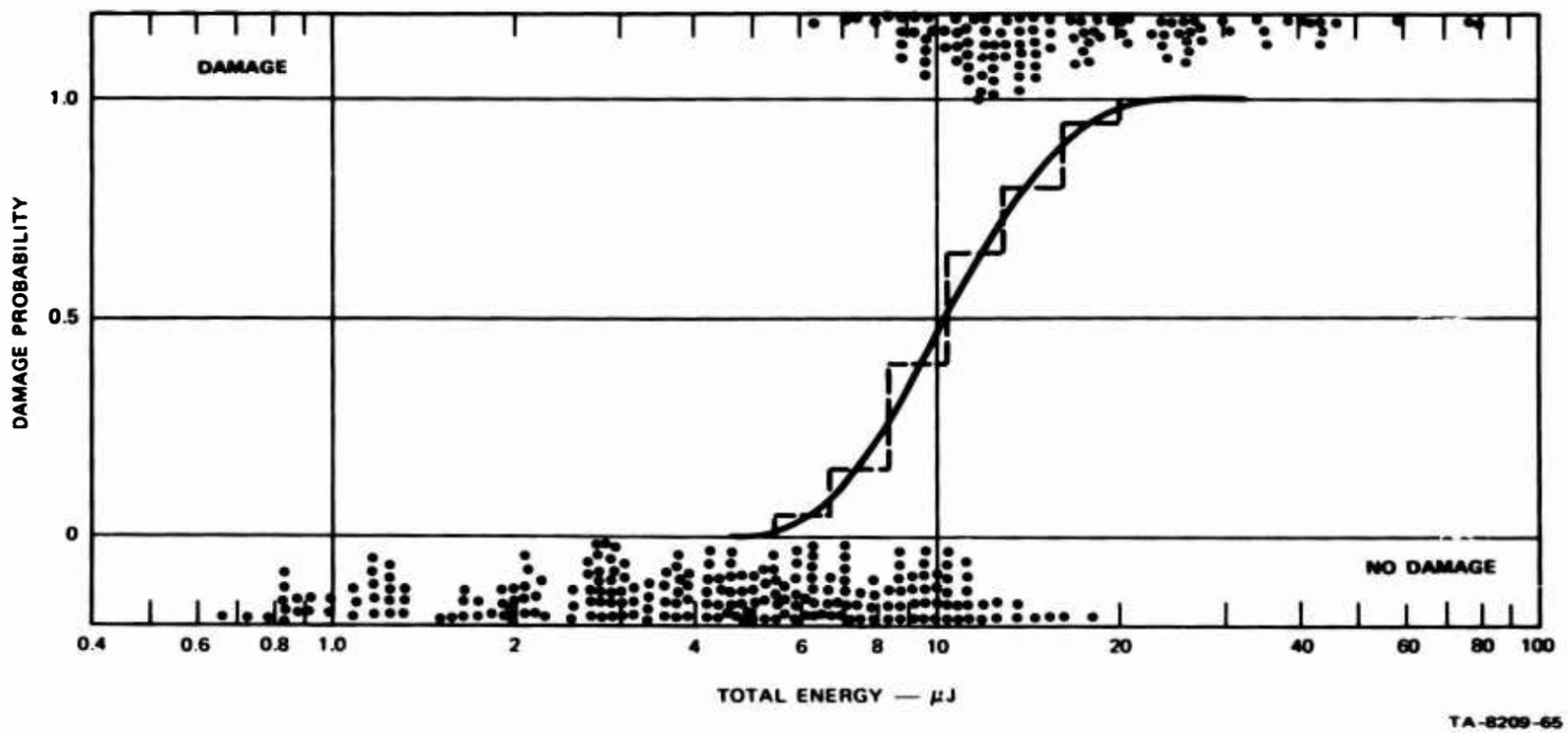

FIGURE 3 PARAMACULAR DAMAGE TO RHESUS MONKEY RETINA WITH DOUBLED Q-SWITCHED NEODYMIUM

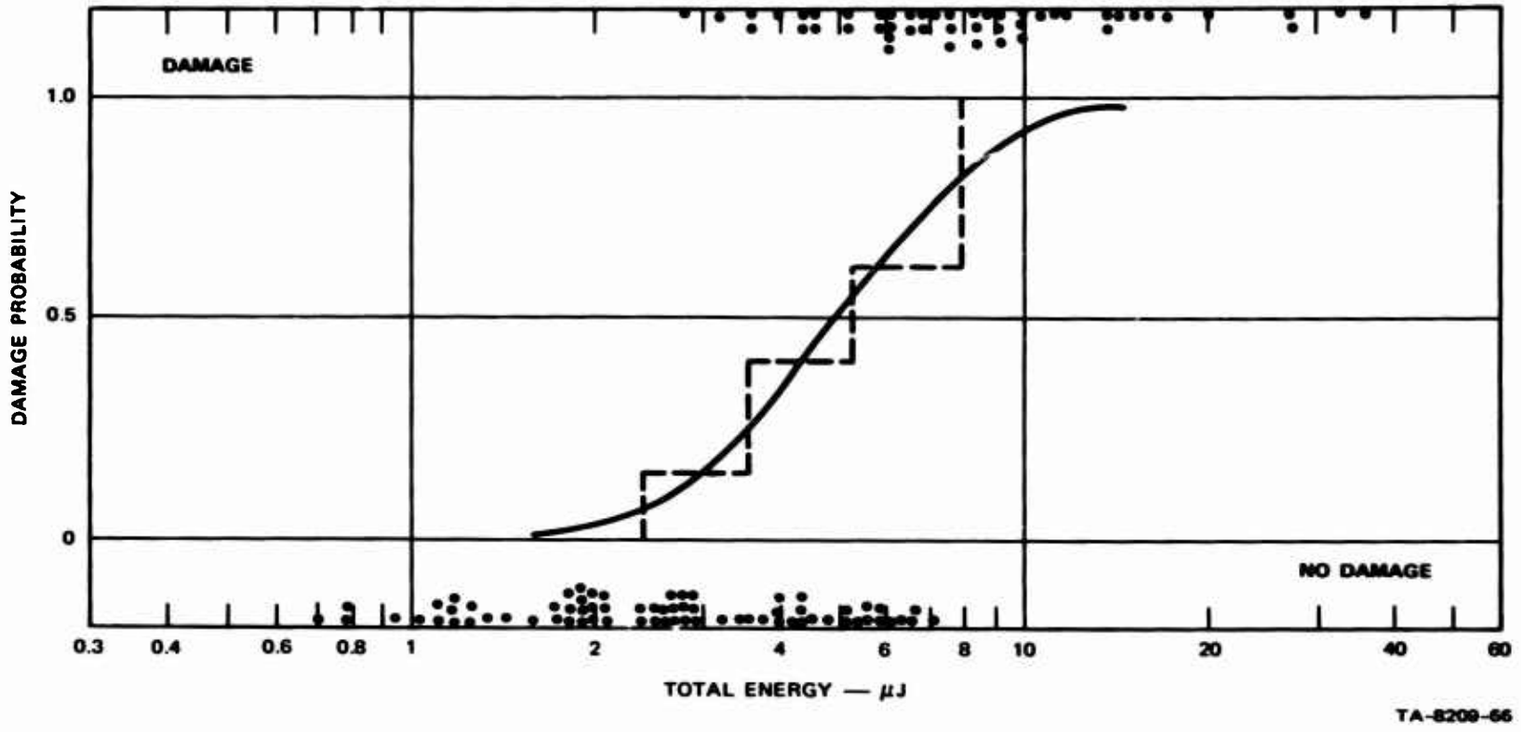

FIGURE 4 MACULAR DAMAGE TO RHESUS MONKEY RETINA WITH DOUBLED Q-SWITCHED NEODYMIUM

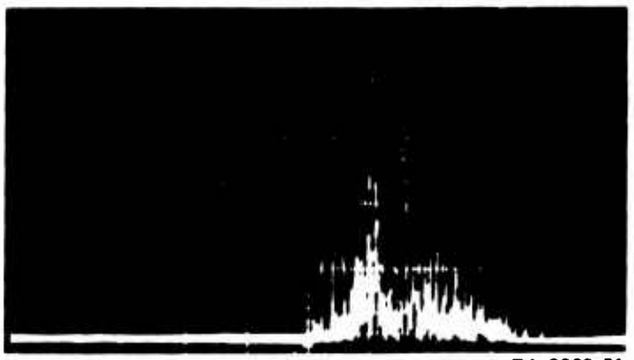

FIGURE 5 TYPICAL PULSE TRAIN OF LONG-PULSED NEODYMIUM LASER

The output beam was reduced in diameter by a factor of about 3.5 by the use of two lenses, in order to obtain higher power density and thus increase conversion efficiency. The beam was then passed through an ADP crystal, with which the 530 nm radiation was obtained. The conversion efficiency in the doubler was not very good. Considerable difficulty was experienced in optimizing the doubled output. It was found necessary to incorporate an accurate thermal control over the laser rod. With a system that maintained the rod to within 0.6° C it was possible to obtain reproducible results, and the crystal could be tuned. A compromise was established between the point of maximum output and the point where variations of temperature had minimal effect on the output.

The doubled laser was located approximately 12 feet away from the delivery system. This was necessary in order to obtain sufficient energy in the eye to cause minimal damage.

Even though the laser/doubler combination was close to the delivery station, the beam was relatively well collimated, because of the critical phase-matching requirement in the doubling crystal. The beam divergence was measured to be 2 mrad. Thus, the spot size in the retina for rhesus monkeys would be larger than 27 μ, depending on the eye optics.

2. Experiments and Results

Because of the difficulties in obtaining sufficient doubled output and the fact that the doubling crystal was being damaged, it was decided to keep the number of exposures to a minimum. The paramacular exposures were all placed within the temporal superior and inferior vessel arcades. Thus, the exposures were in the immediate neighborhood of the macula and near the posterior pole. Since the primary interest is in the macular threshold level, there were four paramacular exposures and four macular exposures in each eye.

The procedure used was similar to that used in the Q-switched case discussed above. The appearance of the retinal lesions at threshold and above threshold is similar to that reported previously for other lasers.[2,3]

The experimental results presented in this section are a summary of the data on 20 rhesus monkeys. The data are presented separately as macular and paramacular. The data for the paramacular area are summarized in Figure 6. The data show that the 50-percent probability for damage occurs at about 74 μJ. The macular data summarized in Figure 7 show a 50-percent probability for damage of about 38 μJ. This is appreciably lower than the paramacular area. This same trend has been observed for a number of the lasers[3-4] as well as for doubled Q-switched neodymium discussed in the previous section.

D. Doubled Q-Switched Ruby

1. Laser Characteristics

The laser makes use of a 6-inch-by-1/2-inch ruby rod with Brewster-angle cuts. The rod is pumped by two 12-mm-bore linear flash lamps in a close-coupled geometry. The lamps are air-cooled, whereas

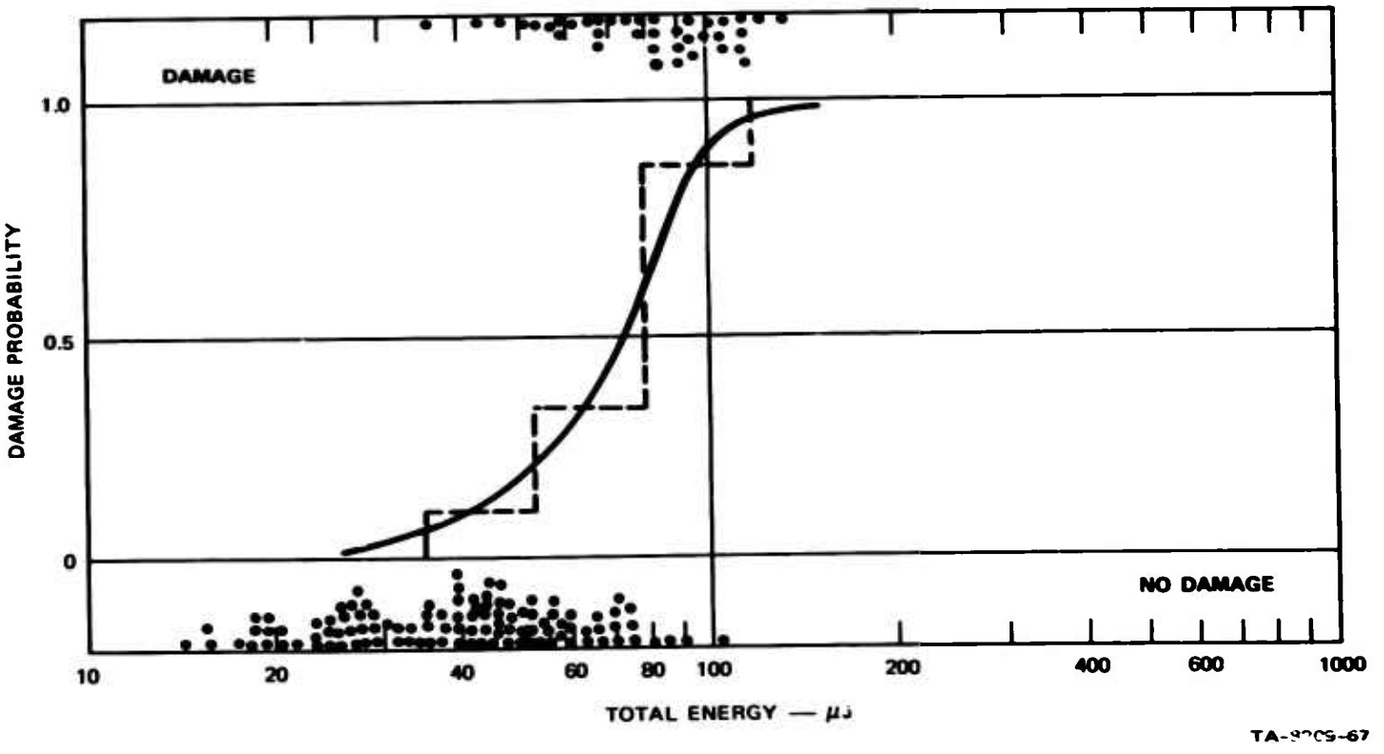

FIGURE 6 PARAMACULAR DAMAGE TO RHESUS MONKEY RETINA WITH DOUBLED LONG-PULSED NEODYMIUM

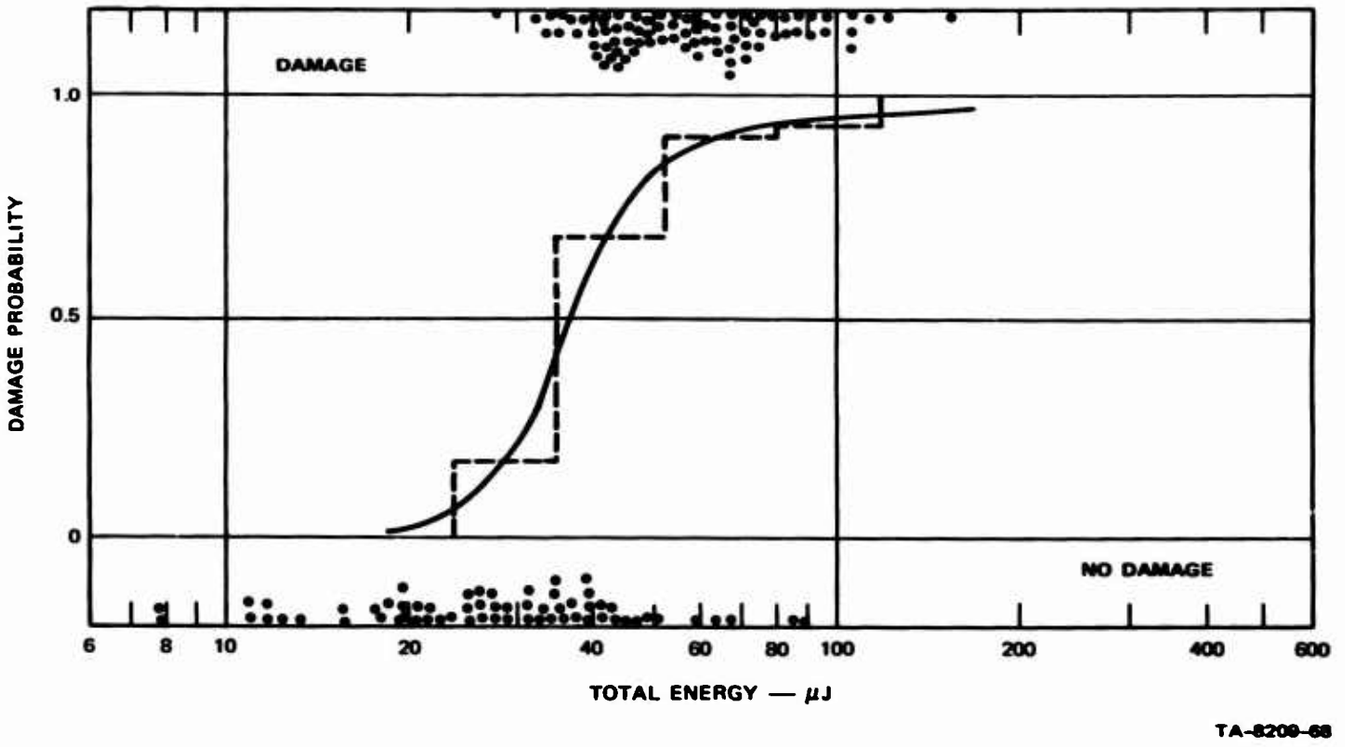

FIGURE 7 MACULAR DAMAGE TO RHESUS MONKEY RETINA WITH DOUBLED LONG-PULSED NEODYMIUM

the ruby rod is water-cooled. The laser is Q-switched with a spinning quartz prism revolving at 500 rps. Typically, the output-pulse energy of the ruby laser at 694 nm is 1 J and the pulse length is 30 ns

The output of the laser was introduced immediately into a properly oriented ADP crystal which doubled the ruby frequency, and a pulse was obtained at 347 nm. Immediately after the doubler a filter was used to pass only the doubled output and absorb the fundamental ruby wavelength. A photograph of a typical pulse is shown in Figure 8.

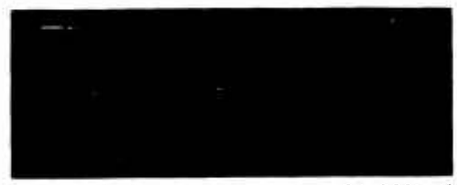

TA 8209 /2

FIGURE 8 TYPICAL OUTPUT PULSE OF Q-SWITCHED RUBY LASER

The doubled laser was located 35 feet from the delivery system. The beam divergence measured for this laser was 1.5 mrad. Thus, when properly focused in the rhesus monkey eye the retinal spot size would be larger than 20 μ, depending on the eye optics.

For the lens-damage experiments, the size of the focused spot provided by the quartz lens that was used was estimated to be 80 μ in diameter.

2. Retinal Experiments and Results

The doubled ruby laser was used in a retinal threshold study. The exposures in rhesus eyes were all placed within the temporal superior and inferior arcades. Thus all exposures were either in the macula or in the immediate neighborhood of the macula.

The procedure was similar to that used in previous experiments. Thus, the criterion for damage was the requirement for an ophthalmoscopically visible response within one hour after exposure.

A total of eight rhesus monkeys were used for these experiments--i.e., a total of sixteen eyes. In half of the eyes, the exposures were made with the proper correction lens located in front of the eye. In the other half of the eyes, a negative lens of approximately 2.5 diopters was included in front of the eye. This lens was used to correct for the refractive power of the eye at 347 nm, which is much higher than the value obtained with retinoscopy, as estimated from calculations.

In all these exposures, no retinal damage was observed. The data are summarized in Figure 9, where it is seen that up to the highest energy values that were used--i.e., somewhat over 6 mJ--no visible response was observed in the retina.

3. Lens-Damage Experiments and Results

The doubled ruby laser was also used to study lens damage in the rhesus monkey in order to determine a threshold level.

The rhesus monkey eyes were dilated maximally by application of atropine prior to the day of the experiment. The laser beam was then focused by the use of a quartz lens of approximately 2-inch focal length. The focused beam was aimed at the edge of the lens near the iris at four well separated locations. Thus, each eye received four exposures in the lens. Each eye was examined carefully under a slit-lamp immediately after exposure and at one month and at three months post-exposure.

A total of 25 animals were used in this study of lens damage, and the results discussed below are a summary of these exposures.

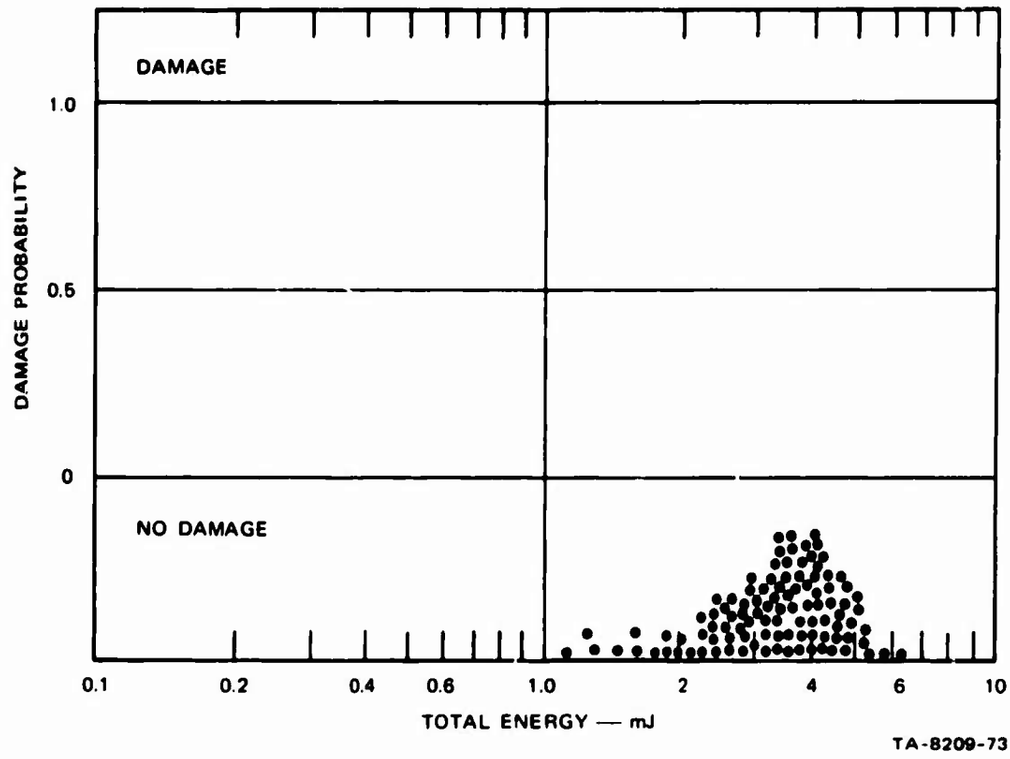

FIGURE 9 SUMMARY OF RETINAL EXPOSURES OF RHESUS MONKEYS TO DOUBLED Q-SWITCHED RUBY

The lenticular damage observed consisted of small areas of opacification--initially very tenuous and difficult to photograph. At the end of one month, however, the opacities appeared considerably more well defined and in some cases considerably larger than was thought to be the exposed area. The appearance of the opacities in detail show small white granules dispersed throughout the damaged area. Some examples of the opacities taken at one and three months post-exposure are shown in Figures 10 through 13. It will be noted that there is considerable difference in the sizes of the lesions. It must be noted that all these are considerably above the threshold level.

The data based on the immediately post-operative observation are summarized in Figure 14. The data for 3-month post-exposure examination are summarized in Figure 15. Statistically, the threshold level did

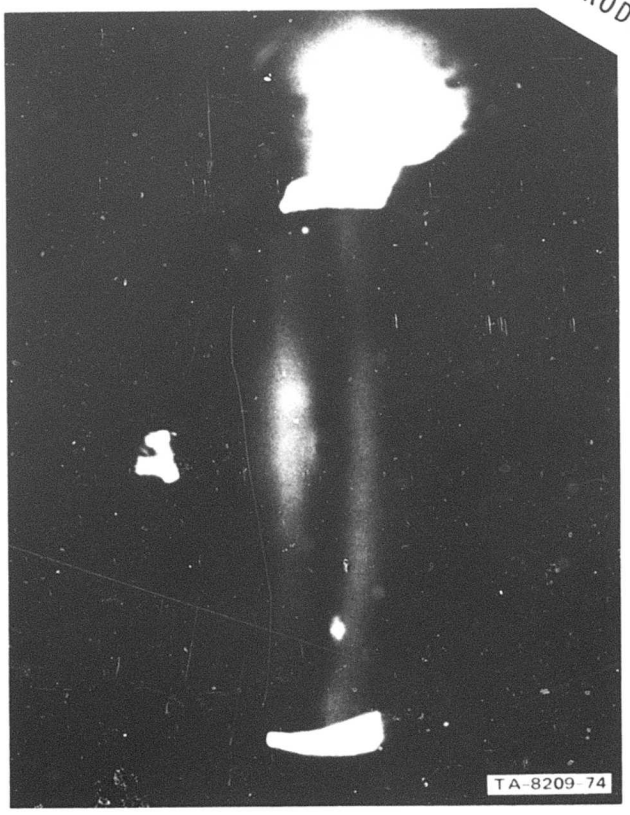

FIGURE 10 SMALL LENS OPACITIES IN RHESUS MONKEY ONE MONTH AFTER EXPOSURE TO DOUBLED Q-SWITCHED RUBY

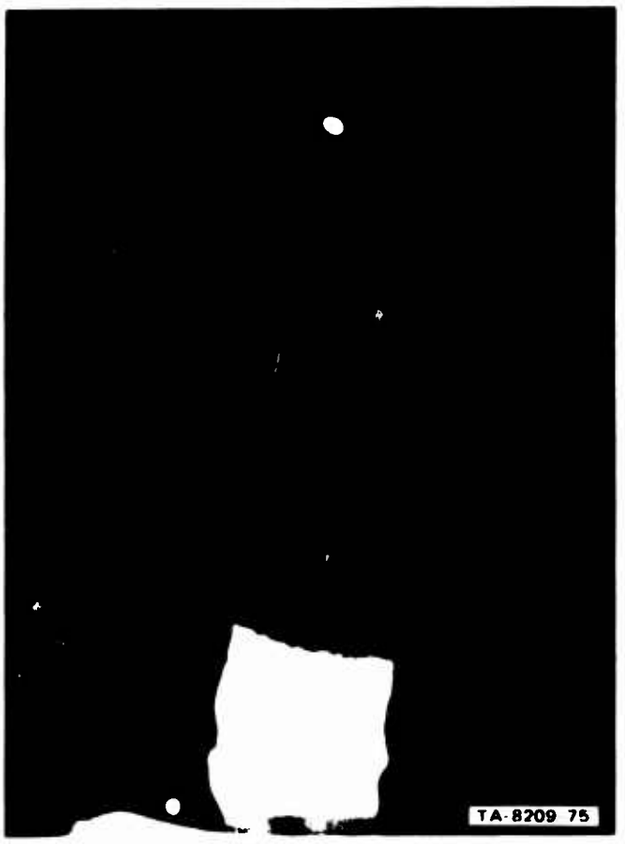

FIGURE 11 RHESUS MONKEY LENS OPACITIES ONE MONTH AFTER EXPOSURE TO DOUBLED Q-SWITCHED RUBY

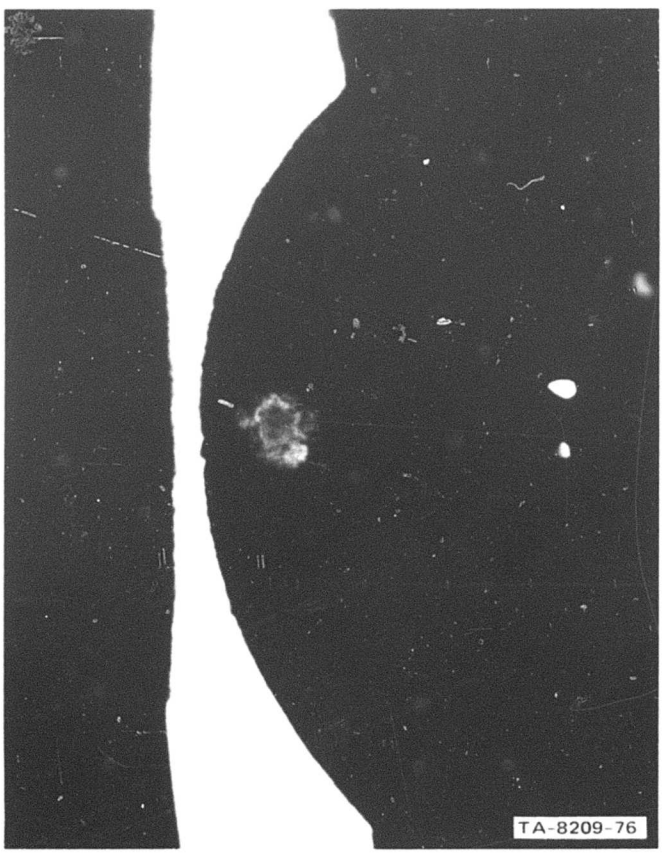

FIGURE 12 RHESUS MONKEY LENS OPACITY THREE MONTHS AFTER EXPOSURE TO DOUBLED Q-SWITCHED RUBY

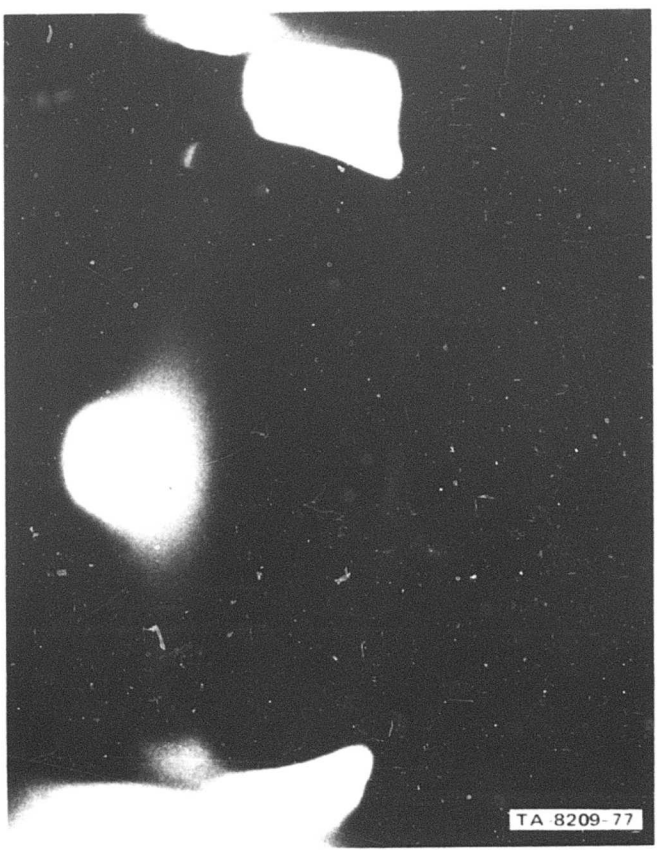

FIGURE 13 POSTERIOR SURFACE LENS CHANGE IN RHESUS MONKEY AFTER DOUBLED RUBY LASER EXPOSURE

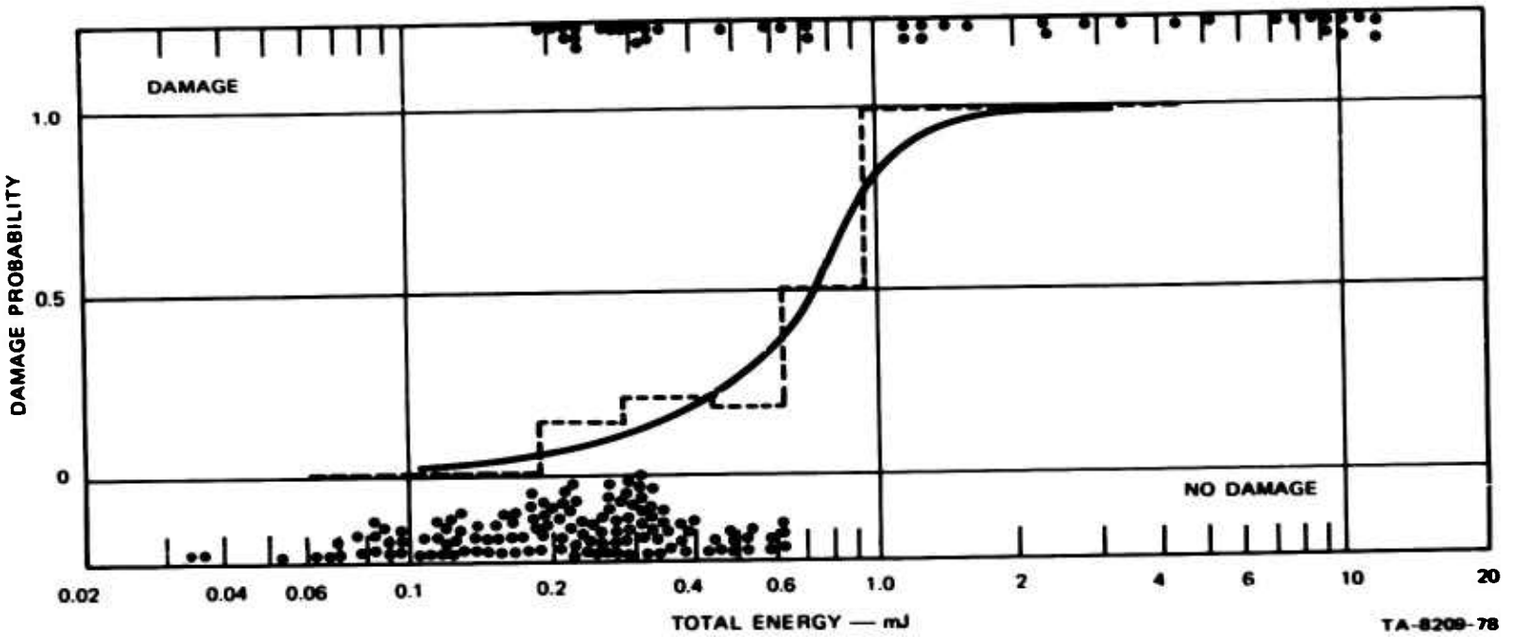

FIGURE 14 RHESUS MONKEY LENTICULAR DAMAGE BASED ON IMMEDIATE POST-OPERATIVE OBSERVATION FOR EXPOSURE TO DOUBLED Q-SWITCHED RUBY

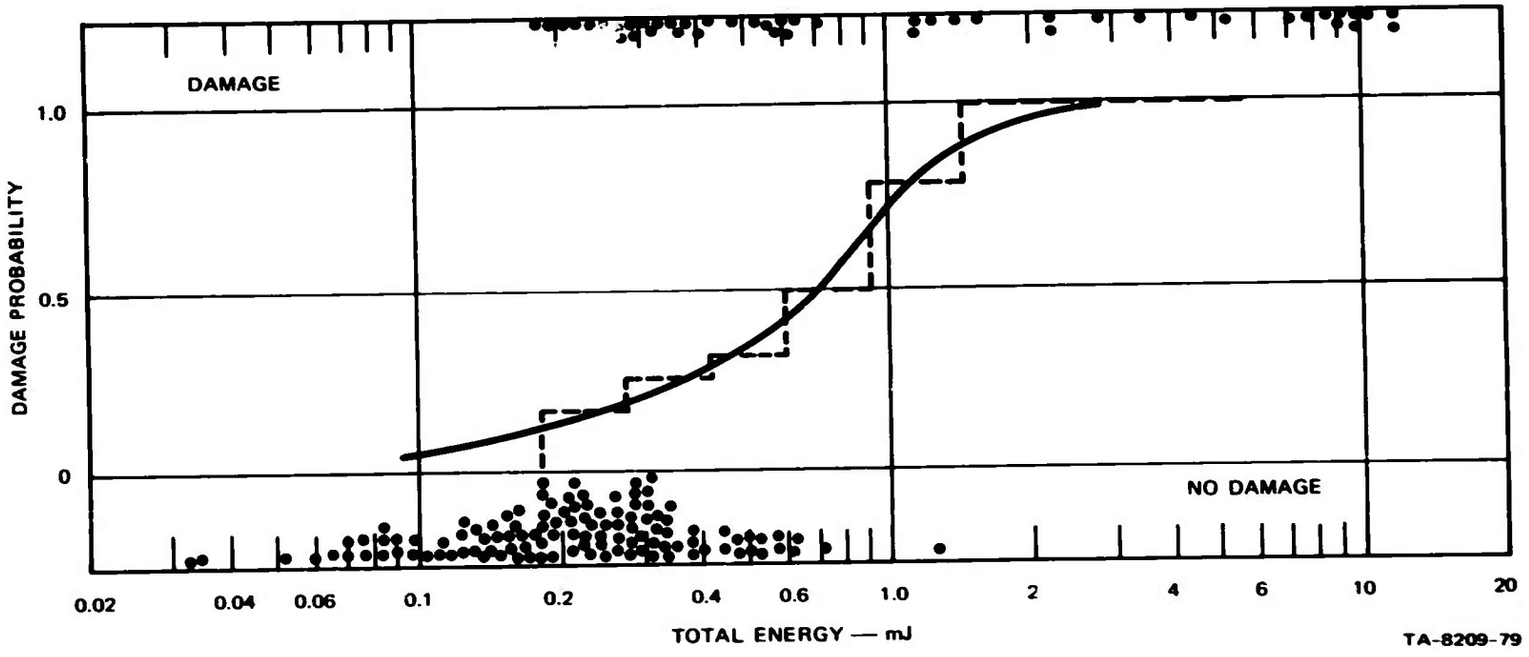

FIGURE 15 RHESUS MONKEY LENTICULAR DAMAGE BASED ON THREE-MONTH POST-OPERATIVE OBSERVATION FOR EXPOSURE TO DOUBLED Q-SWITCHED RUBY

not change appreciably. Thus, although some damage sites that were seen at later examination were not seen immediately, there were also some that were not seen in later examinations although they were marginally observed earlier.

It is noted that the 50-percent probability for damage in these experiments was approximately 0.7 mJ. This is equivalent to 14 J/cm^2 at the site of the exposure.

III THEORETICAL CONSIDERATIONS OF RETINAL DAMAGE

A. Absorption of Light in the Fundus

In the visible and near infrared parts of the spectrum the ocular media are relatively transparent, and thus light is transmitted effectively to the back, or fundus, of the eye. The light arriving at the retina at a high level of illumination passes through the various layers of the retina virtually unattenuated so that a high percentage of the light incident on the cornea reaches the pigment epithelium, the first absorbing layer in the fundus. The highest absorption per unit volume takes place in this layer.

The high absorption of the pigment epithelium layer is due to the high concentration of melanin granules that are located in the pigment epithelium cells. These granules are ellipsoids and spheres in the range of 1/2 to 1 μ in diameter. It is usually noted that these granules are located in the anterior part of the pigment epithelium cells. Thus, although the pigment epithelium cells are approximately 10 μ in thickness, the melanin granules are located within a 3-to-4-μ-thick band immediately adjacent to the outer extremities of the rods and cones.

An appreciable fraction of the light is absorbed by the pigment epithelium. The majority, however, proceeds to the choroid, where it is scattered and partly absorbed by the pigment granules and hemoglobin are present in the choroid. The light that is not absorbed by the choroid proceeds to the sclera.

B. Thermal Damage

Although the processes associated with vision are photochemical in nature, the retinal damage caused by intense sources of light is generally understood to be thermal in nature. This, at least, appears to be true for damage associated with acute exposures lasting up to tens of seconds. Thus, the light that is absorbed by the pigment epithelium and choroid is converted into heat. Consequently, if the intensity is high enough the temperature rise of the absorbing tissues can be sufficient to cause thermal damage.

The normal operation of a living cell requires that the ambient temperature be kept within very restrictive limits. It is not surprising, therefore, that a relatively small increase in temperature can lead to damaging consequences. Many theories have been proposed as to how thermal damage of the cell takes place. Among the current theories are that damage is due to alterations of nucleic acids, inactivation of enzymes, or denaturation of proteins.[5]

These inactivation and denaturation processes must be analyzed as rate processes. Just as heat speeds up chemical reactions, a small temperature rise can profoundly influence the rate of the inactivation or denaturation processes. Thus, in model calculations, some consideration must be given not only to the thermal history of the tissues but also the rate processes that are involved.

C. Models for Retinal Damage

The first attempt at a theory for retinal burns was developed by Vos.[6] He assumed a thin (10-μ-thick) rectangular region absorbing uniformly, and calculated the thermal history of the exposed site. He considered times that were longer than 20 ms and spot sizes that were greater

than 180 μ. Vos concluded that the retinal damage indicated by data of Ham et al.[7] was closely associated with the calculated amount of steam formation produced by the exposure. He did point out, however, that damage should occur at lower levels of irradiation since albumins begin to coagulate at temperatures between 45° C and 60° C.

Subsequently, Ham et al.[8] developed a model in which heat was generated uniformly in the pigment epithelium and in the choroid. More recently Clarke et al.[9] reported on a model in which pigment epithelium and choroid were assumed to act as uniform absorbers. In the latter case only a steady-state model was treated. Another analysis of thermal damage, also for steady-state condition, was made by Hansen et al.,[10] who considered a steady-state solution of a cylindrical volume of uniform heat generation representing the pigment epithelium.

All these models have shortcomings and difficulties, and comparison with experimental data has not been satisfactory. None of the models takes into account a rate equation for the denaturation or inactivation process. In the following sections we consider a simple model in order to make calculations to compare with recent experimental damage data for CW lasers.

D. Temperature Variation in Retinal Exposures

In this section we consider a simple model for calculating the temperature rise at the center of a retinal exposure to intense radiation. We consider the time regime in which thermal relaxation plays a strong role. These arguments would thus be most appropriate for exposures to CW lasers.

We assume that the beam that is incident on the retina has variations only in the radial direction. Two cases are considered: first, the

intensity is assumed uniform and of radius a, and second, a gaussian distribution is assumed.

The absorption is assumed to take place in two layers, the first representing the pigment epithelium and the second representing the choroid. It is of interest then to calculate the temperature on the axis, since the highest temperature will occur somewhere on the axis. For any point on the axis the temperature rise can be calculated as the sum of the contributions from the pigment epithelium layer and from the choroid.

As shown in the Appendix, the solution for an absorbing layer of thickness 2ℓ is given by Eq. (A-12) as

$$\psi(\vec{r},t) = \frac{u_0 \kappa}{2} \int_0^t d\tau \left\{ \operatorname{erfc} \frac{z - \ell}{2\sqrt{\kappa\tau}} - \operatorname{erfc} \frac{z + \ell}{2\sqrt{\kappa\tau}} \right\} \left(1 - e^{-\frac{a^2}{4\kappa\tau}} \right) \qquad (1)$$

for a uniform beam of radius a. For a beam of gaussian distribution it is shown by Eq. (A-14) that the temperature rise is given by:

$$\psi(\vec{r},t) = \frac{u_0 \kappa}{2} \int_0^t d\tau \left\{ \operatorname{erfc} \frac{z - \ell}{2\sqrt{\kappa\tau}} - \operatorname{erfc} \frac{z + \ell}{2\sqrt{\kappa\tau}} \right\} \left\{ \frac{1}{1 + \frac{4\kappa\tau}{a^2}} \right\} \qquad (2)$$

where the radial distribution is given by

$$f(r) = e^{-\left(\frac{r}{a}\right)^2} \quad . \qquad (3)$$

In Eqs. (1) and (2),

$$\kappa = \text{Diffusivity } (\text{cm}^2/\text{s})$$

and

$$u_0 = \frac{P_0 \beta}{(2\ell)4.18\ K} \qquad (4)$$

where

P_0 = Power density (watts/cm^2)

K = Heat conductivity (cal cm/cm^2-s-°C)

β = Fraction of power absorbed.

Extensive computer calculations were made for ψ, defined in Eqs. (1) and (2), using dimensionless variables defined by

$$X = \frac{z}{\ell} \qquad A = \frac{a}{\ell}$$

$$T = \frac{2}{\ell}\sqrt{\kappa t} \tag{5}$$

$$\Psi = \frac{4\psi}{u_0 \ell^2} \quad .$$

Results were obtained for a number of parameter variations so that various spot sizes and choroid and pigment epithelium configurations could be selected. Some of the results are plotted in Figures 16 and 17 for the uniform beam cross section, and in Figures 18 and 19 for the gaussian beam cross section.

Before applying the simple thermal model to experimental configurations so that a comparison with the empirical data can be made, thermal damage of biological material is discussed in the next section.

E. Thermal Rate Processes

The denaturation of proteins and the inactivation of enzymes must be analyzed as a rate process. As shown by observations of rates of chemical reactions, the empirical expression for the reaction rate constant has the form

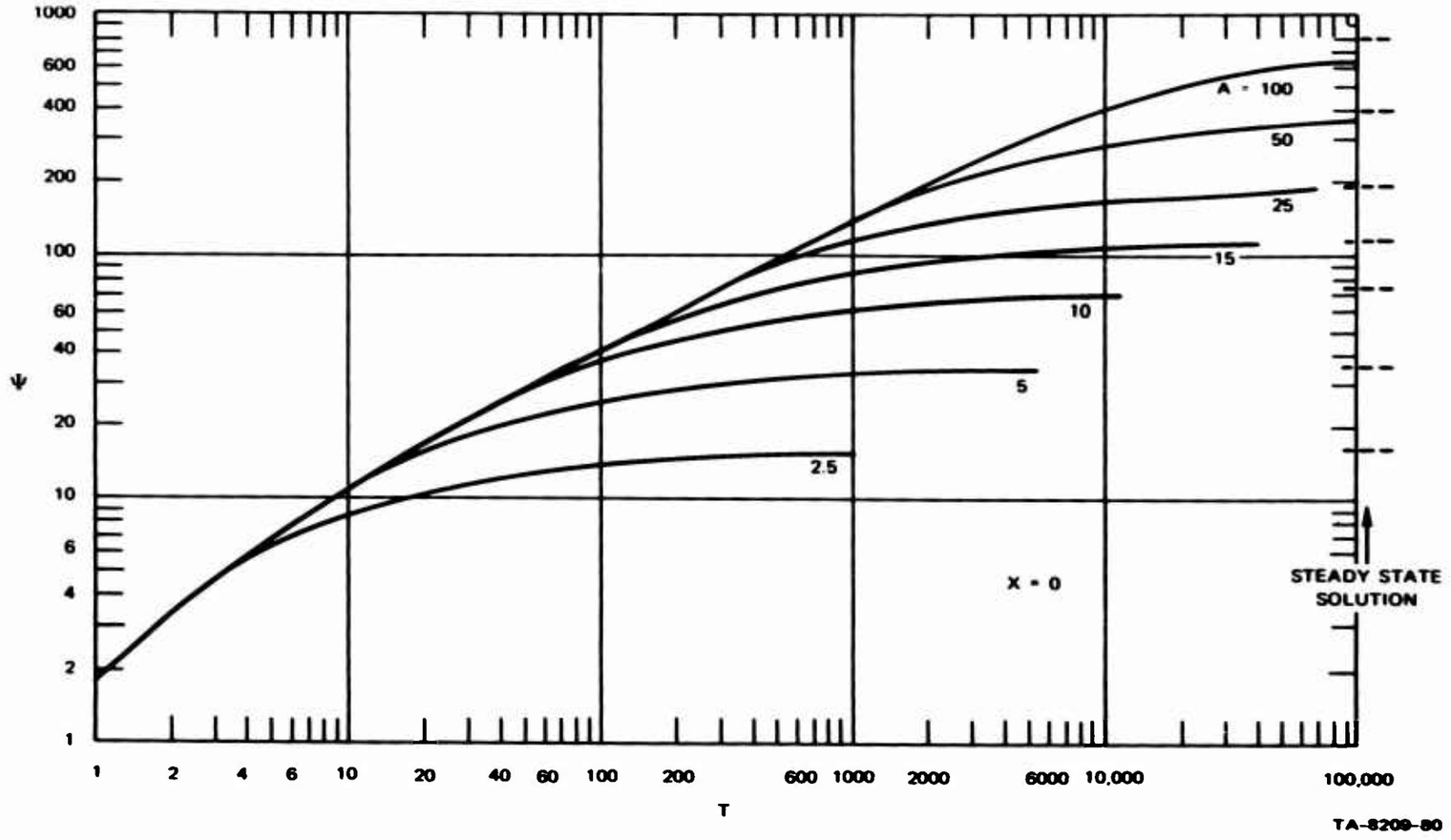

FIGURE 16 TEMPERATURE RISE AS A FUNCTION OF TIME FOR VARIOUS SPOT SIZES AT THE CENTER OF AN ABSORBING DISC — UNIFORM BEAM CROSS SECTION

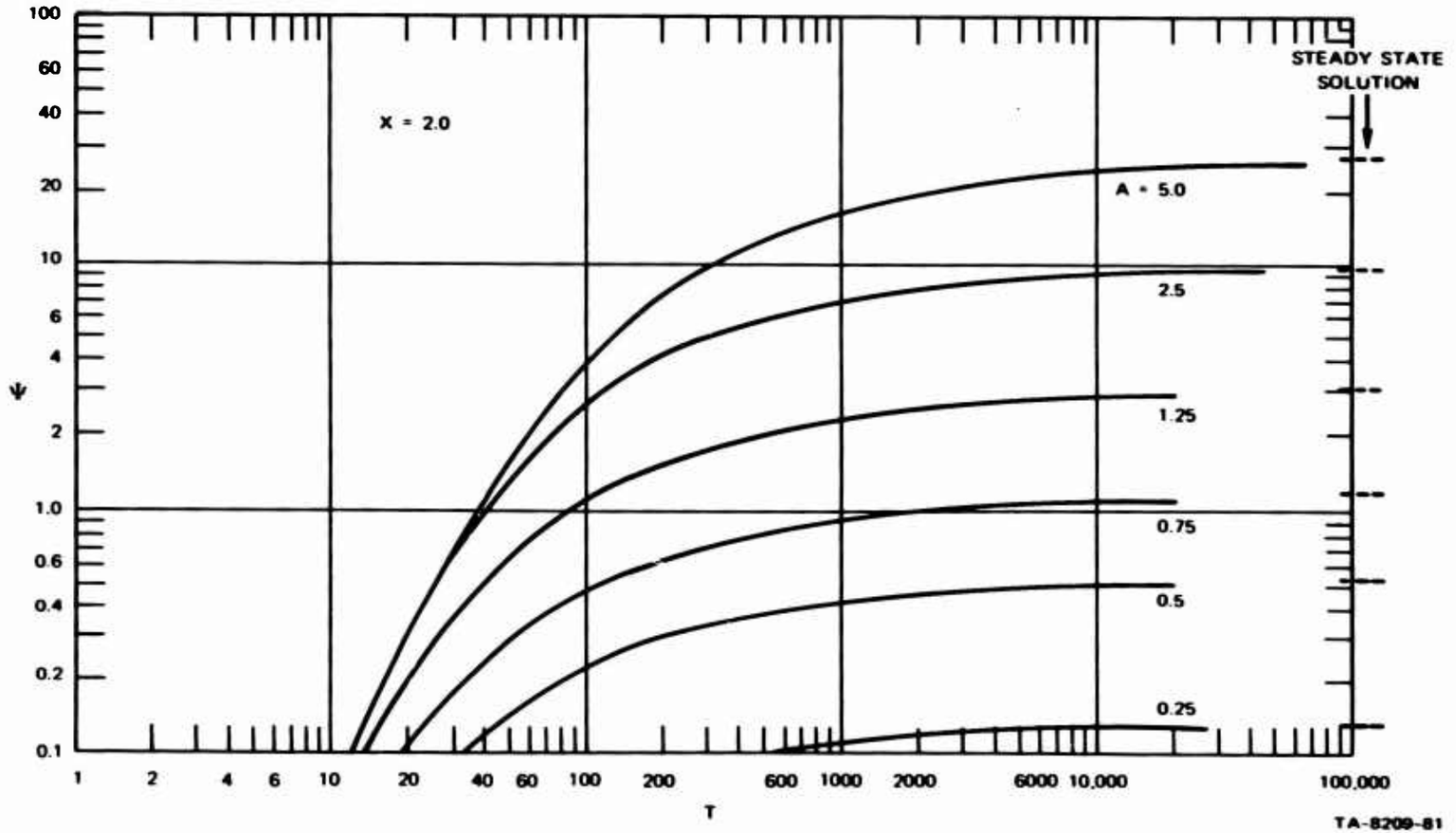

FIGURE 17 TEMPERATURE RISE AS A FUNCTION OF TIME FOR VARIOUS DISTANCES FROM CENTER OF A DISC — UNIFORM BEAM CROSS SECTION

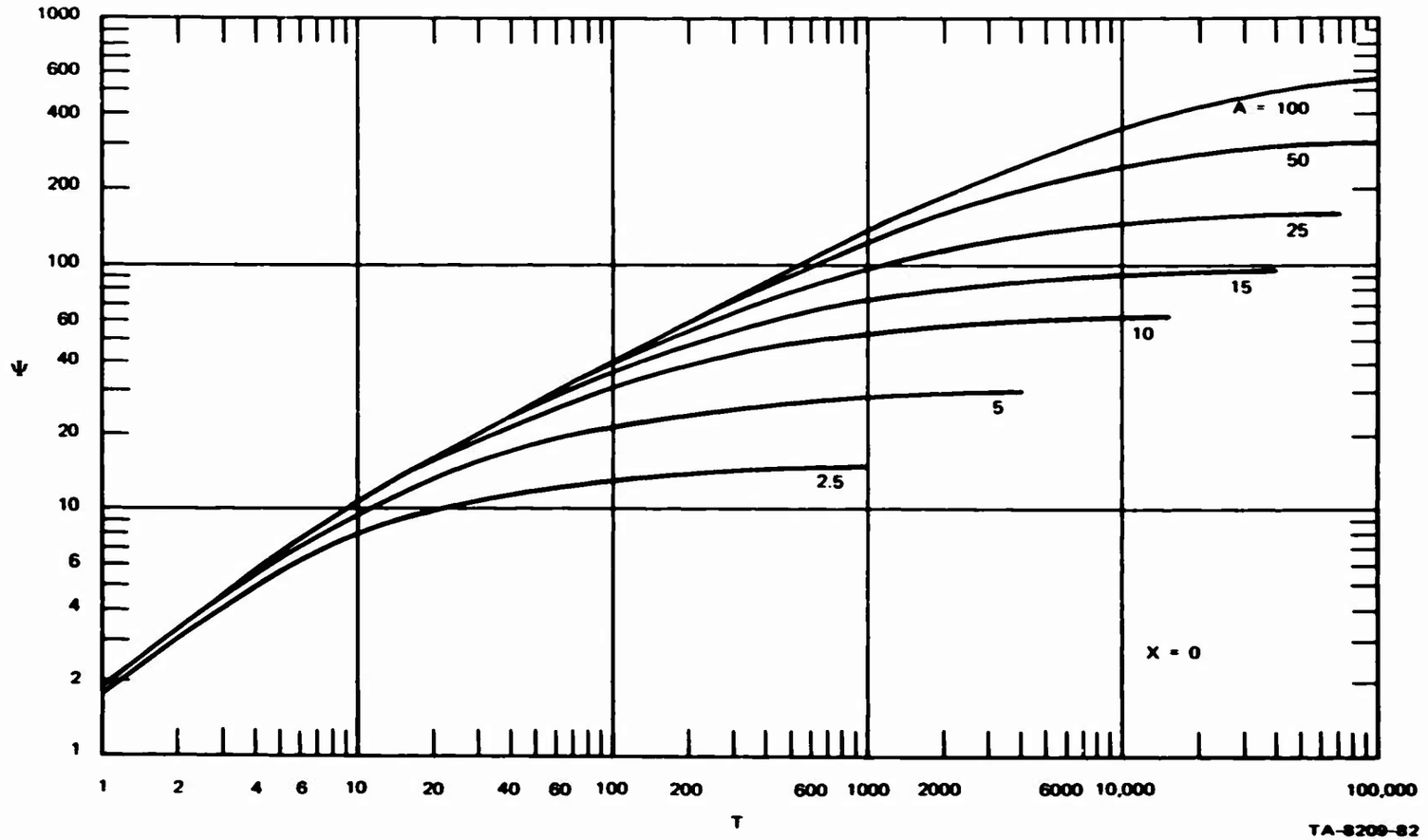

FIGURE 18 TEMPERATURE RISE AS A FUNCTION OF TIME FOR VARIOUS SPOT SIZES AT CENTER OF ABSORBING DISC — GAUSSIAN BEAM CROSS SECTION

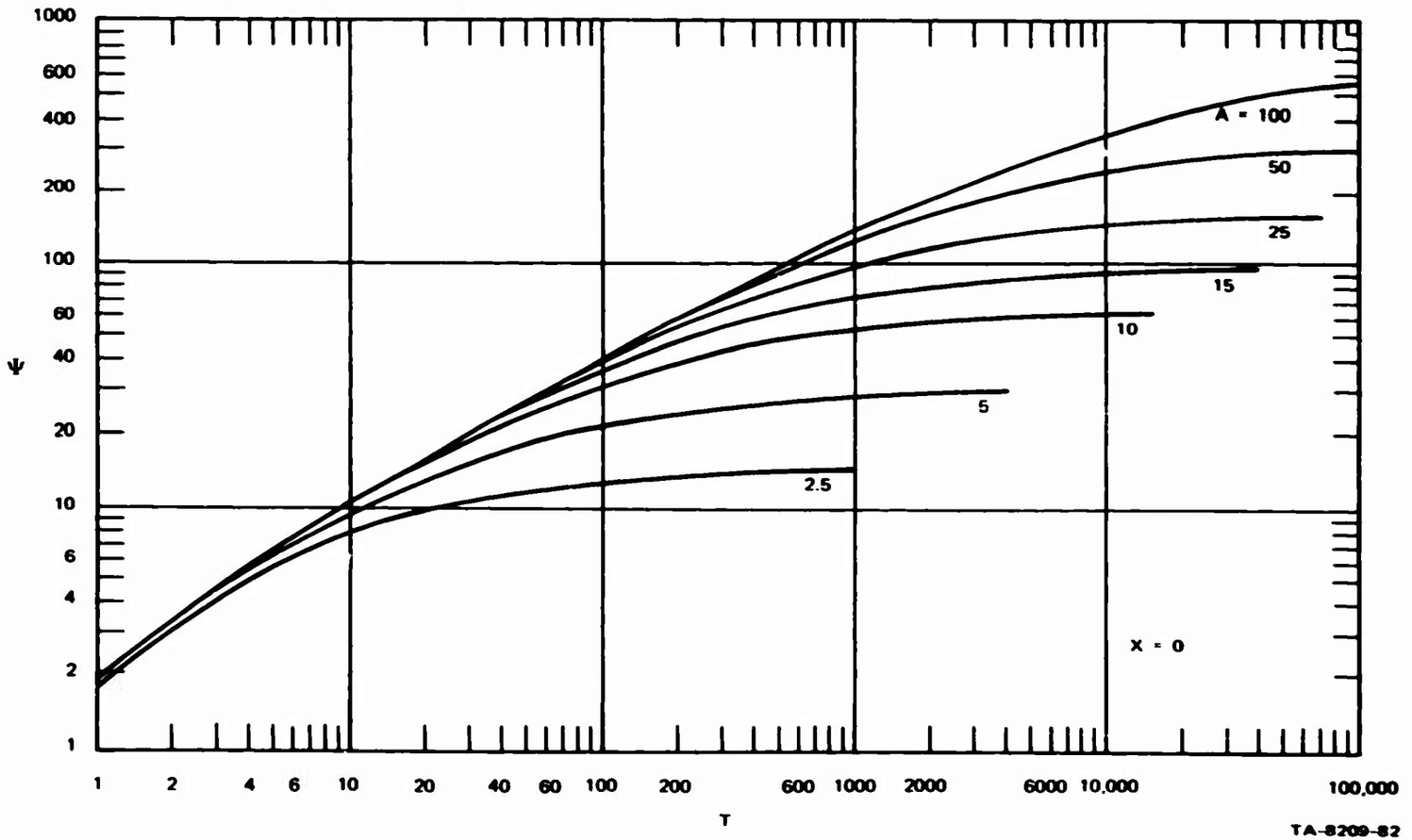

FIGURE 18 TEMPERATURE RISE AS A FUNCTION OF TIME FOR VARIOUS SPOT SIZES AT CENTER OF ABSORBING DISC — GAUSSIAN BEAM CROSS SECTION

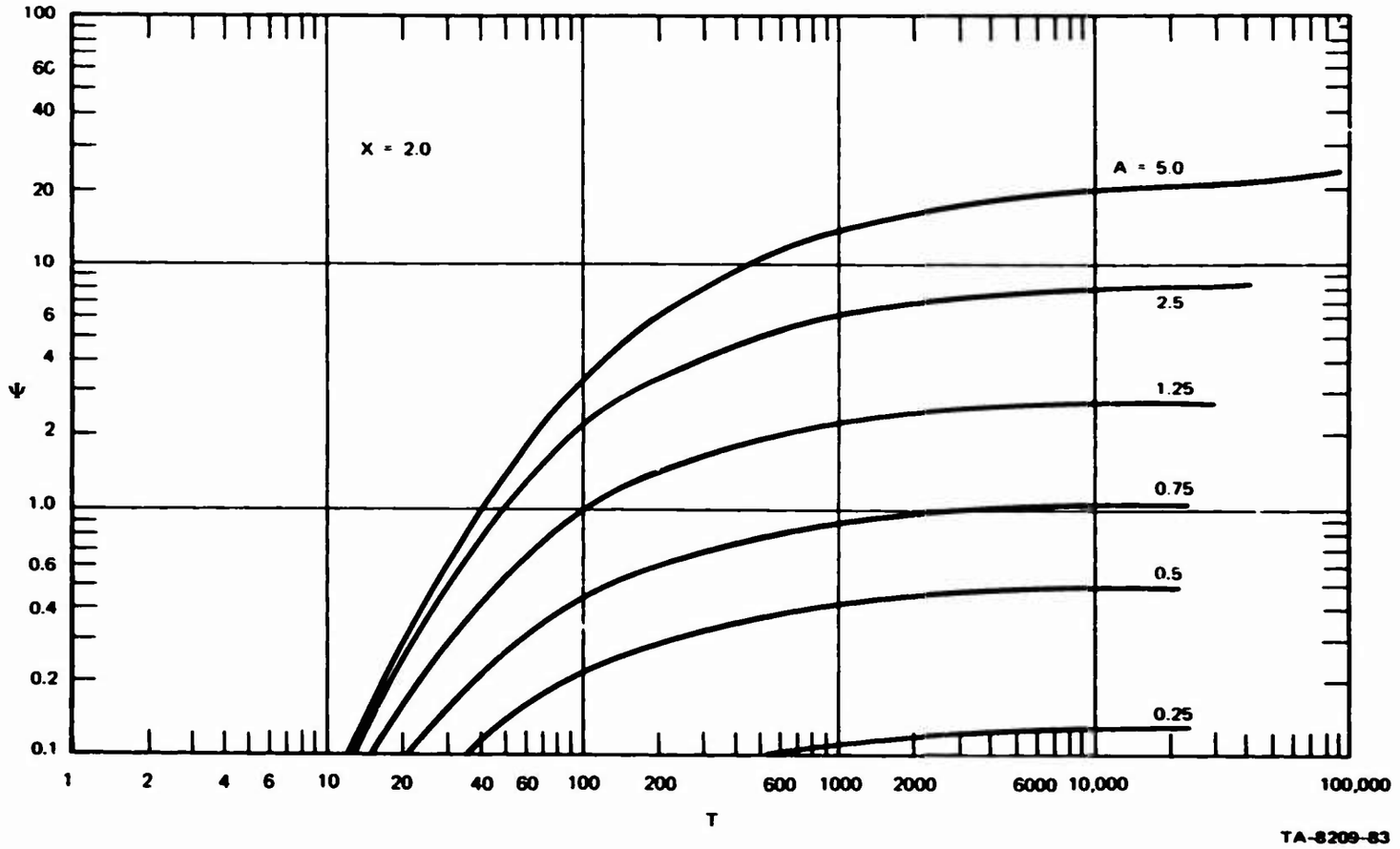

FIGURE 19 TEMPERATURE RISE AS A FUNCTION OF TIME FOR VARIOUS DISTANCES FROM CENTER OF DISC — GAUSSIAN BEAM CROSS SECTION

$$\frac{d}{dT}(\ell n\ k') = \frac{E_0}{RT^2} \quad . \tag{6}$$

This can also be written as

$$k' = A\, e^{-\frac{E_0}{RT}} \quad . \tag{7}$$

In a similar way, from statistical mechanics treatments[11] it can be shown that the reaction rate is given by

$$k' = \frac{kT}{h} e^{-\frac{\Delta F^{\ddagger}}{RT}} = \frac{kT}{h} e^{\frac{\Delta S^{\ddagger}}{R}} e^{-\frac{\Delta H^{\ddagger}}{RT}} \tag{8}$$

where k is the Boltzmann constant, h is Planck's constant, $\Delta F^{\ddagger}$ is the change in activation free energy, $\Delta H^{\ddagger}$ the change in heat energy, and $\Delta S^{\ddagger}$ the change in entropy.

This may be rewritten as

$$\frac{d}{dT}(\ell n\ k') = \frac{\Delta H^{\ddagger} + RT}{RT^2} \tag{9}$$

which is seen to be similar to the Arrhenius equation, Eq. (6), if we identify E_0 with $(\Delta H^{\ddagger} + RT)$. Since the influence of temperature on the reaction rate is dominated by the exponential factor, although A (Eq. 7) does vary slightly with temperature, it is usual to assume that A is independent of temperature in the treatment of experimental data.

The reaction associated with denaturation of proteins and inactivation of enzymes is usually unimolecular;[12] thus the reaction follows first-order kinetics, and we can write

$$\frac{dC}{dt} = k'C \tag{10}$$

where C is the concentration.

The surviving fraction S may then be expressed as

$$S = \frac{C}{C_0} = e^{-\int k' dt} \tag{11}$$

or

$$\ell n\ S = -\int k' dt \quad . \tag{12}$$

In terms of the temperature rise in tissues ψ we therefore must consider the equation

$$\ell n\ S(\vec{r},t) = \ell n \frac{C(\vec{r},t)}{C_0(\vec{r})} = -\int_0^t A\, e^{-\frac{E_0}{R[T_o+\psi(\vec{r},t)]}}\, dt \tag{13}$$

where T_o is the ambient temperature and ψ is the temperature rise due to the radiation being absorbed by the medium.

In comparing the theoretical results with the experimental data it must be kept in mind that the experimental results usually involve a gross examination of the exposed site and it is unknown what the survival fraction is when damage is observed. However, since the solution of Eq. (13) is relatively insensitive to the survival fraction that is used, we can select arbitrarily a value for $C/C_0 = 1/e$.

Thus, the solution of Eq. (13) in the form

$$\int_0^{\tau} A\, e^{-\frac{E_0}{R[T_o+\psi(t)]}}\, dt = 1 \tag{14}$$

must be obtained for the temperature rise, ψ, given by the thermal conduction model.

F. Comparison of Theory and Experimental Results

In this section we consider the application of simple thermal models to the understanding of experimental retinal threshold data obtained with CW lasers. The experimental threshold data that are examined were obtained using an argon CW laser in rhesus monkey eyes.

The data shown in Figure 20 represent threshold data for an argon laser.[3] Each point on the plot represents the 50-percent probability for damage value, and is a result of a large number of exposures in rhesus monkey eyes. The data accumulated were based on an ophthalmoscopically visible criterion. Two features of the data shown in Figure 20 are of interest. First it is noted that the curves continue to decrease as a function of the length of the exposure. This trend is much more pronounced than would be expected from the constant-temperature thermal-damage model that is usually referred to in thermal-damage discussions.

The second feature noted in the data shown in Figure 20 is that the spacing between the curves does not follow the simple relationship expected from simple model considerations. Thus, the data for the different spot sizes fall much closer together than would be predicted from simple-model arguments.

We turn now to a discussion of the first feature--the shape of the damage-threshold curves. We consider the data for the 30-μ retinal spot, and present calculations for a number of simple models to indicate the trends observed.

First, a simple one-layer absorbing model is used to simulate the pigment epithelium (PE) absorption. Thus, the beam is assumed to be

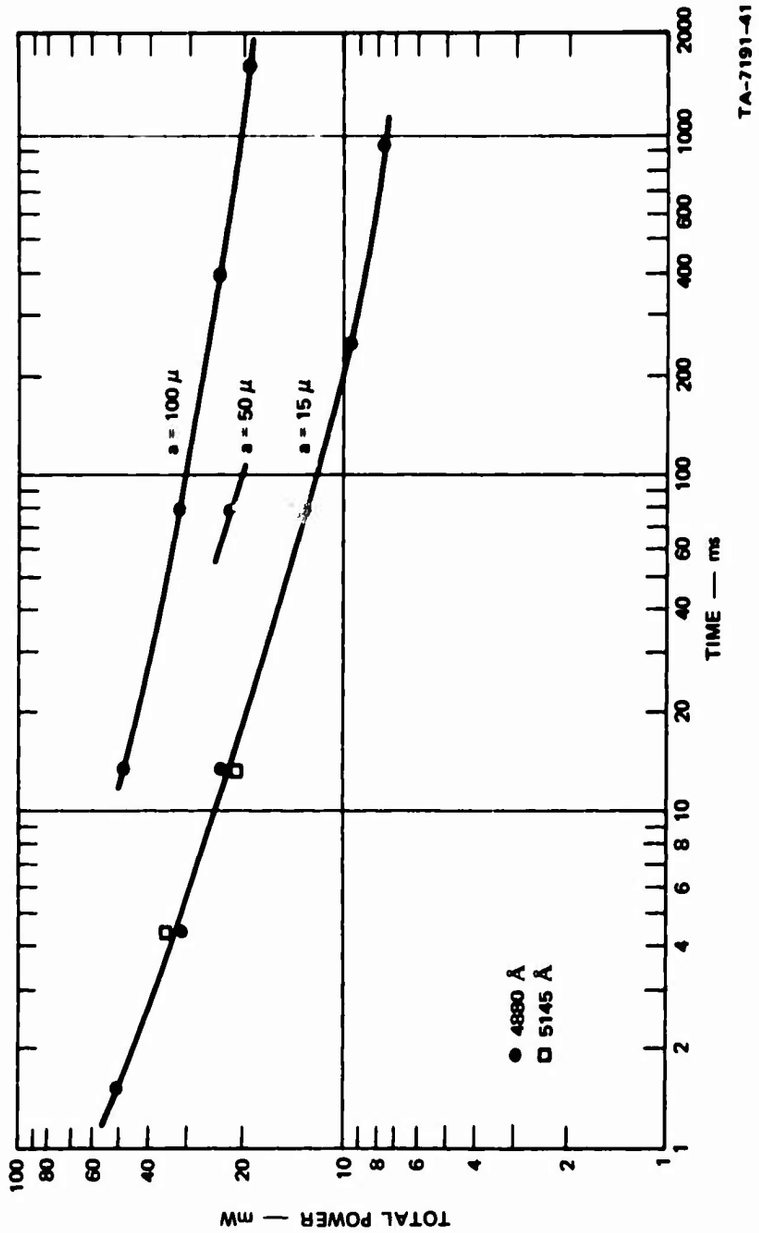

FIGURE 20 THRESHOLD RETINAL DAMAGE IN RHESUS MONKEY FOR ARGON LASER

absorbed only in the pigment epithelium, and the temperature at the center of the PE is calculated. The PE layer is assumed to be 4 μ in thickness, which, it is felt, realistically represents the absorbing part of the layer. Using the curves of Figure 16 and Eqs. (4) and (5) we find that the threshold variation for this simple model must have the form shown in Figure 21. The curve has been arbitrarily shown to match

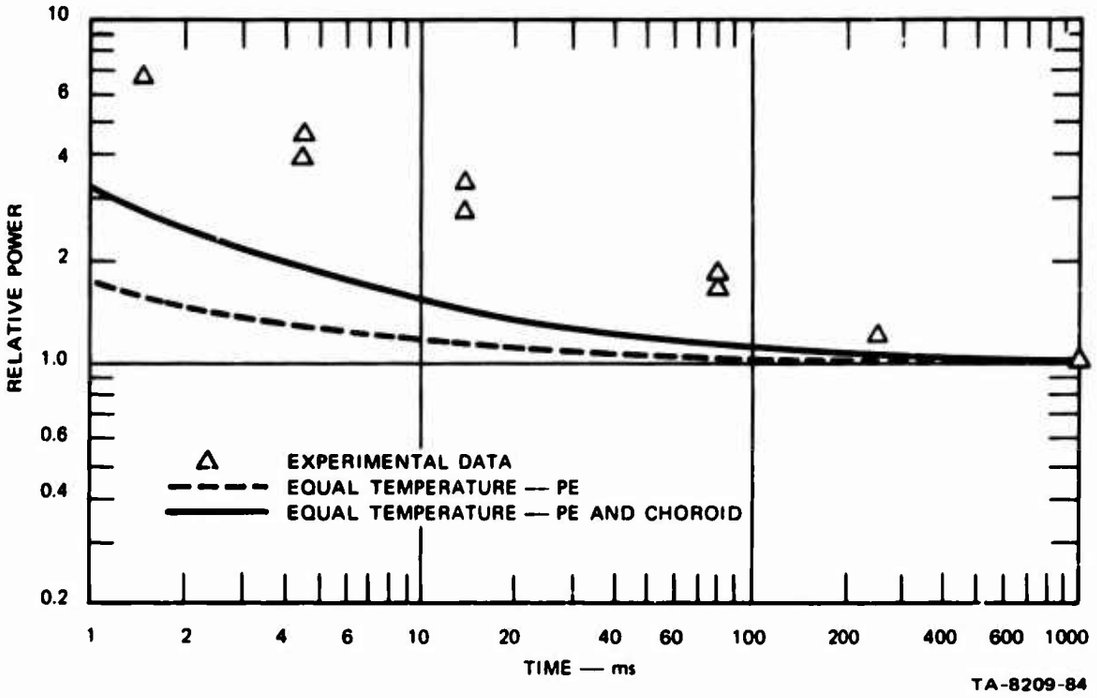

FIGURE 21 COMPARISON OF RELATIVE SHAPE OF THRESHOLD VARIATION FOR SIMPLE MODEL WITH ACTUAL DATA — ASSUMING ONLY PIGMENT EPITHELIUM LAYER ABSORBING AND PE AND CHOROID EQUALLY ABSORBING

the experimental data at one second. It is apparent that the experimental data show considerably more change with time than would be expected from simple theory. Very little variation is to be noted between a 4-μ and a 10-μ thickness (10 μ is the thickness usually assumed for the PE layer). A comparison between the two is shown in Figure 22.

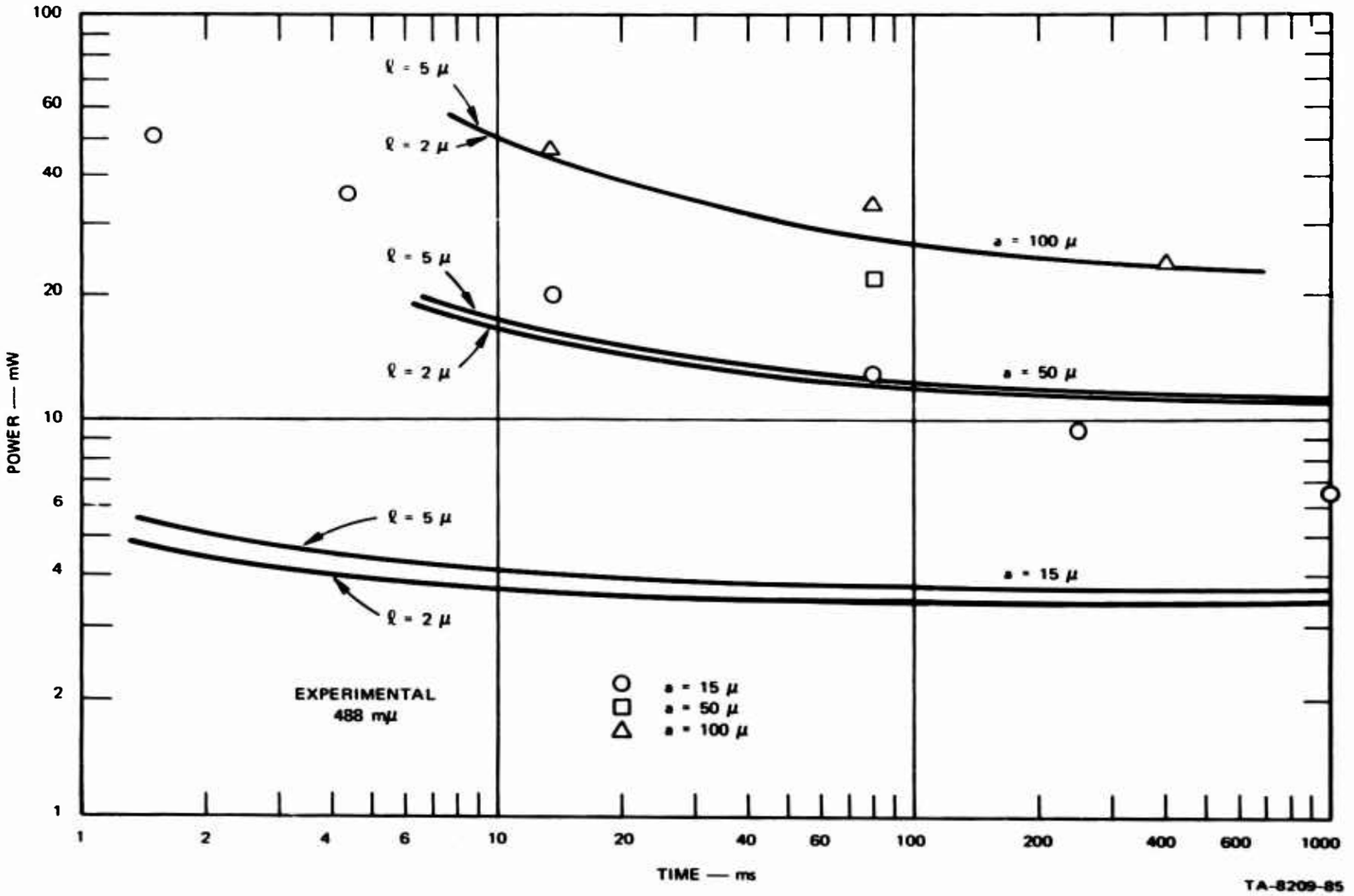

FIGURE 22 COMPARISON OF RELATIVE SHAPE OF THRESHOLD VARIATION FOR TWO THICKNESSES OF THE PIGMENT EPITHELIUM LAYER FOR VARIOUS RETINAL SPOT SIZES

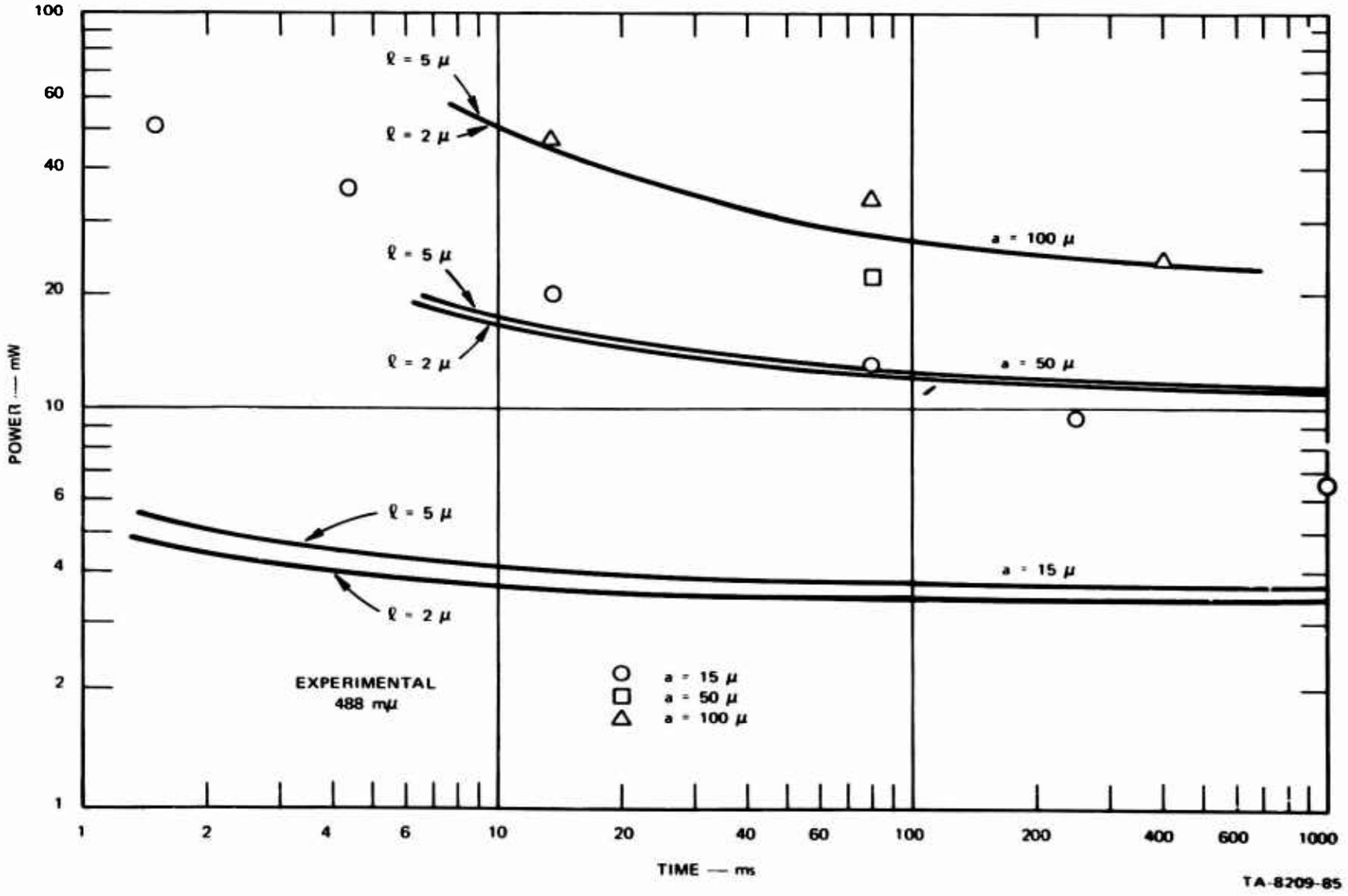

FIGURE 22 COMPARISON OF RELATIVE SHAPE OF THRESHOLD VARIATION FOR TWO THICKNESSES OF THE PIGMENT EPITHELIUM LAYER FOR VARIOUS RETINAL SPOT SIZES

A more complex model was then assumed so as to represent the PE and the choroid more realistically. It is assumed that the choroid absorption layer is 40 μ thick and is centered 30 μ behind the pigment epithelium absorbing layer. It is then assumed that an equal amount of power is absorbed by the PE and by the choroid. A calculation of the threshold power for constant temperature of this model is also shown in Figure 21. Here it is seen that the curve is appreciably closer to the actual experimental curve; however, it is still insufficient to explain the experimental observations. It is to be noted that if the large majority of the power was absorbed by the choroid, the calculated curve could come closer to the experimental observations. This, however, would be contrary to absorption measurements of the various absorbing layers.

We turn now to thermal-damage calculations that model the damage process by considering the rate processes and by solving Eq. (14) for the temperature-rise variation prescribed by the thermal-model calculations.

It was assumed that the fundus consists of two absorbing layers, representing the PE and choroid, that absorb equal amounts of power. Equation (14) was then used to calculate requirements of exposure time for a number of inactivation energies, E_o, as a function of input-power levels. Figure 23 shows examples for E_o = 50,000, 70,000, and 100,000 cal/mole, which represents a range of values typical of low inactivation energies for proteins and enzymes. A visual fit of these curves with the experimental data showed that the curve for E_o = 70,000 cal/mole gave a good fit. This is shown in Figure 24, where the agreement is seen to be excellent. It must be kept in mind, however, that this match depends on the absorbing model that is chosen--i.e., the relative absorption between the PE and the choroid influences the value of E_o that is calculated. Thus, a more accurate knowledge of the absorption of the PE and choroid

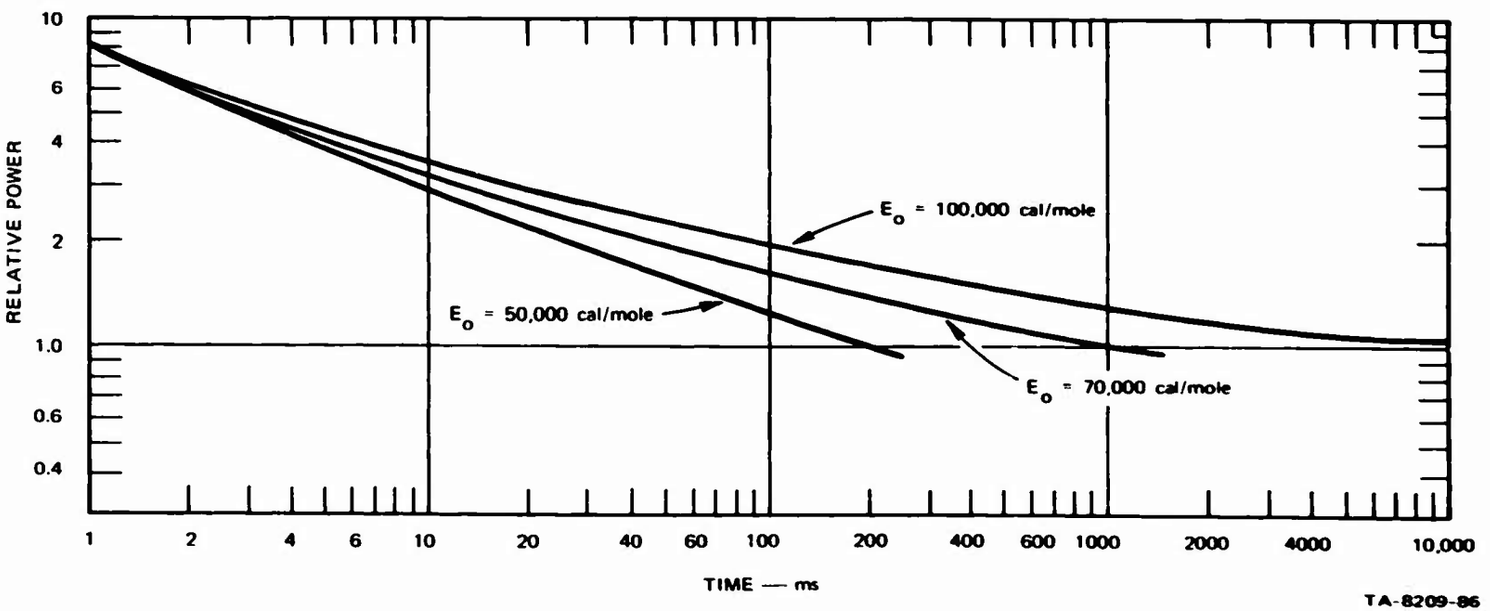

FIGURE 23 RELATIVE THRESHOLD VARIATIONS FOR THREE INACTIVATION ENERGIES

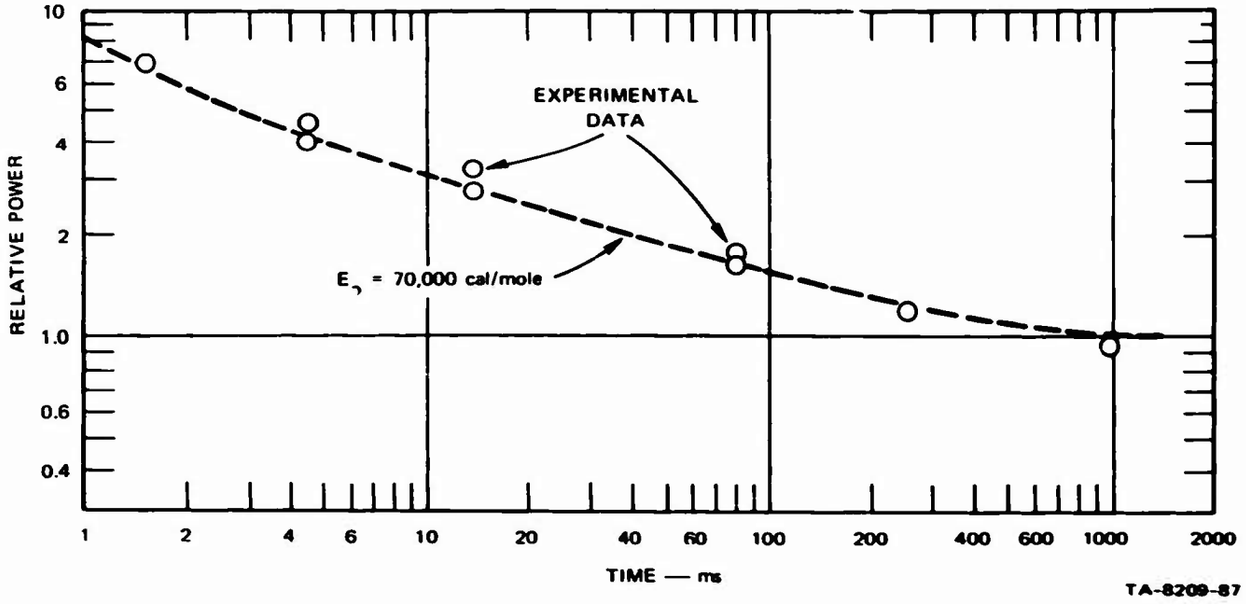

FIGURE 24 COMPARISON OF RELATIVE SHAPE OF THRESHOLD VARIATION FOR INACTIVATION THERMAL MODEL WITH EXPERIMENTAL DATA. E_o = 50,000 cal/mole. PE AND CHOROID ASSUMED EQUALLY ABSORBING.

would be necessary before an accurate value of E_o could be determined and an identification of a particular enzyme or protein could be made.

Finally, we consider the problem of variation of threshold with spot size. From the calculations of temperature shown in Figures 16 through 19 we obtain values for the power level required to reach the same temperature at each spot size, at a time of 80 ms, where we have three experimental data points. Calculations were made for the simple PE model as well as the two-layer PE and choroid model. The relative power levels required are shown in Figure 25, where for each curve the

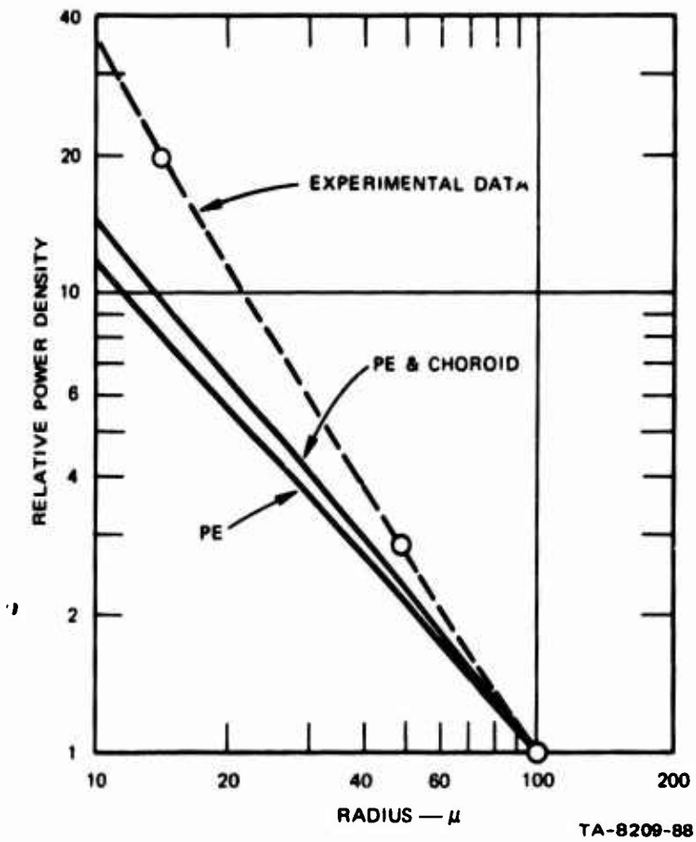

FIGURE 25 COMPARISON OF SIMPLE MODELS — RELATIVE SHAPE OF THRESHOLD VARIATION AS A FUNCTION OF SPOT SIZE

normalization is made arbitrarily to the 200-μ spot size. It is apparent that there is considerable discrepancy between the theory and the experimental data. Although the addition of the choroid does bring the calculation closer to the experiment, choroid absorption much higher than the PE absorption would be required to bring the calculation and the experimental data closer together.

Application of the inactivation-rate-process calculations would not move the theoretical curves appreciably closer to the experimental points; thus there appears to be a need for a nonthermal explanation of this phenomenon. As mentioned earlier,[3,13] the most reasonable explanation may be that the effect is due to the scattering of the ocular refracting surfaces and media.

IV CONCLUSIONS

Threshold levels for retinal damage were reported for rhesus monkeys for a doubled Q-switched neodymium laser. The threshold was found to be 10 μJ, which is lower than for Q-switched ruby. The macular area was found to be approximately twice as sensitive as the paramacular area.

Threshold data for doubled long-pulsed neodymium were taken, and a threshold of 74 μJ was found to be approximately seven times higher than for the Q-switched mode.

Threshold data for retinal damage for the doubled Q-switched ruby laser produced no visible damage up to levels of 6 mJ. Thus, the absorption by the ocular media does increase the threshold at 347 mμ considerably. Threshold data on lenticular damage gave a value of approximately 14 J/cm^2 as the required incident level to cause damage. This is not to say that lens damage will occur before retinal damage occurs at this wavelength.

Theoretical models for retinal damage were discussed and computer parametric calculations were presented. Comparison of calculated threshold values with experimental data has shown some disagreement with simple thermal models. It was shown that the experimental variation of threshold with spot size is inconsistent with simple thermal models. In addition, it was shown that the experimentally observed variation of threshold with time could not be explained by simple thermal models. However, it was shown that the time variations observed in the experimental data are consistent with a theory that describes the denaturation or inactivation process of the damage mechanism with an appropriate rate equation.

ACKNOWLEDGMENTS

The authors gratefully acknowledge the valuable contributions of Ann Hammond, James Hayes, and George Paris, M.D. in the animal threshold experiments.

Appendix

HEAT-FLOW PROBLEM

The conduction of heat in an isotropic solid is described by the following equation:

$$\frac{\partial \psi}{\partial t} = \kappa \nabla^2 \psi - \frac{\kappa}{K} Q(\vec{r}, t) \qquad \text{(A-1)}$$

where

ψ = Temperature rise (°C)

$\kappa = K/\rho C$ = Diffusivity (cm^2/s)

K = Heat conductivity (cal cm/cm^2-5° C)

ρ = Density (gr/cm^2)

C = Heat capacity (cal/gr °C)

Q = Heat-generating density ($cal/s\text{-}cm^3$)

t = Time (s).

In situations where heat is generated by absorption from an electromagnetic wave, the heat-generating density can most conveniently be expressed in terms of the absorption of an incident flux P ($watts/cm^2$), where the absorption by the medium may be expressed in terms of the absorption coefficient.

If it is assumed that a plane wave is propagating in the z direction, then the power density in the medium will be given by:

$$P = P_0 e^{-\alpha z} f(t)$$

$$Q = -\frac{\partial P}{\partial \tau} = \frac{\alpha P_0}{4.18} e^{-\alpha z} f(t) \qquad (cal/s\text{-}cm^2) \quad . \qquad (A\text{-}2)$$

In a simpler model that we will consider below, it is assumed that the absorbing layer absorbs uniformly. If the depth of the layer is taken to be 2ℓ, then the heat-generating density is given by:

$$Q = \frac{P_0 \beta}{4.18\ (2\ell)} f(t) \qquad (A\text{-}3)$$

where β is the fraction of the incident power that is absorbed.

The solution of the heat-conduction equation (A-1) in three dimensions is required to handle the thermal processes of the retina during exposure. It is assumed that the radiation is absorbed in small volumes, and that the heat is conducted away in all directions. Thus, we assume that the heat-generating volumes are located in an infinite medium of isotropic properties and of totally uniform temperature as the initial condition.

Equation (A-1) may be rewritten as:

$$\nabla^2 \psi - \frac{1}{\kappa} \frac{\partial \psi}{\partial t} = -u(\vec{r}, t) \qquad (A\text{-}4)$$

where

$$u(\vec{r}, t) = \frac{Q(\vec{r}, t)}{K} \quad .$$

The Green's function for Eq. (1) is

$$g(R, \tau) = \frac{1}{8\sqrt{\kappa}(\pi\tau)^{3/2}} e^{-\frac{R^2}{4\kappa\tau}} U(\tau) \qquad (A\text{-}5)$$

where

$$R = |\vec{r} - \vec{r}'|$$

$$\tau = t - t'.$$

The solution of Eq. (A-4) is

$$\psi(\vec{r},t) = \int_0^t dt' \int u(r',t')G(\vec{r} - \vec{r}', t - t')d^3r'$$

$$= \int_0^t d\tau \int u(\vec{r}, t - \tau)g(R,\tau)d^3r' \quad . \qquad \text{(A-6)}$$

Using Eq. (A-5) in Eq. (A-6) we obtain, for interaction, volumes that are circularly symmetric:

$$\psi(\vec{r},t) = \frac{u_0}{8\sqrt{\kappa\pi}^{3/2}} \int_0^t \frac{d\tau}{\tau^{3/2}} e^{-\frac{r^2}{4\kappa\tau}} \int_0^\infty r'dr' e^{-\frac{r'^2}{4\kappa\tau}} \times f(r')S_\phi S_z \qquad \text{(A-7)}$$

where $f(r')$ is a radial source function, and

$$S_\phi = 2\pi I_0\left(\frac{rr'}{2\kappa\tau}\right) \qquad \text{(A-8)}$$

and

$$S_z = \int_{-\ell}^{\ell} dz' e^{-\frac{(z-z')^2}{4\kappa\tau}}$$

$$= \sqrt{\kappa\pi\tau}\left\{\text{erfc}\,\frac{z - \ell}{2\sqrt{\kappa\tau}} - \text{erfc}\,\frac{z + \ell}{2\sqrt{\kappa\tau}}\right\} \quad . \qquad \text{(A-9)}$$

Substituting Eq. (A-8) and Eq. (A-9) into Eq. (A-7) we obtain:

$$\psi(\vec{r},t) = \frac{u_0}{4} \int_0^t \frac{d\tau}{\tau}\, e^{-\frac{r^2}{4\kappa\tau}}$$

$$\times \left\{ \operatorname{erfc} \frac{z-\ell}{2\sqrt{\kappa\tau}} - \operatorname{erfc} \frac{z+\ell}{2\sqrt{\kappa\tau}} \right\}$$

$$\times \int_0^\infty r'dr'\, e^{-\frac{r'^2}{4\kappa\tau}}\, f(r') I_0\left(\frac{rr'}{2\kappa\tau}\right) \quad . \qquad \text{(A-10)}$$

The special case of interest is the temperature along the axis--i.e., $r = 0$. For this case,

$$I_0\left(\frac{rr'}{2\kappa\tau}\right) = 1 \quad .$$

We consider now two cases:

Case I--Uniform Radial Distribution.

$$f(r') = \begin{cases} 1 & r \le a \\ 0 & r > 0 \end{cases}$$

then

$$\int_0^a r'dr'\, e^{-\frac{r'^2}{4\kappa\tau}} = 2\kappa\tau \left(1 - e^{-\frac{a^2}{4\kappa\tau}}\right) \quad . \qquad \text{(A-11)}$$

Substituting in Eq. (A-10) we obtain:

$$\psi(\vec{r},t) = \frac{u_0 \kappa}{2} \int_0^t d\tau \left\{ \operatorname{erfc} \frac{z-\ell}{2\sqrt{\kappa\tau}} - \operatorname{erfc} \frac{z+\ell}{2\sqrt{\kappa\tau}} \right\} \left(1 - e^{-\frac{a^2}{4\kappa\tau}}\right) \quad . \qquad \text{(A-12)}$$

Case II--Gaussian Radial Distribution.

$$f(r') = e^{-\left(\frac{r'}{a}\right)^2}$$

then

$$\int_0^\infty r'dr' \; e^{-\frac{r'^2}{4\kappa\tau}} \; e^{-\left(\frac{r'}{a}\right)^2} = \frac{2\kappa\tau}{1 + \frac{4\kappa\tau}{a^2}} \quad . \tag{A-13}$$

Substituting into Eq. (A-10) we obtain:

$$\psi(\vec{r}, t) = \frac{u_0 \kappa}{2} \int_0^t d\tau \left\{ \operatorname{erfc} \frac{z - \ell}{2\sqrt{\kappa\tau}} - \operatorname{erfc} \frac{z + \ell}{2\sqrt{\kappa\tau}} \right\} \left\{ \frac{1}{1 + \frac{4\kappa\tau}{a^2}} \right\} \tag{A-14}$$

where, from Eqs. (A-3) and (A-4),

$$u_0 = \frac{P_0 \beta}{(2\ell) 4.18 \; K} \quad . \tag{A-15}$$

REFERENCES

1. A. Vassiliadis et al., "Investigations of Laser Damage to Ocular Tissues," Tech. Report AFAL-TR-67-170, Contract AF 33(615)-3060, SRI Project 5571, Stanford Research Institute, Menlo Park, California (March 1967).

2. A. Vassiliadis et al., "Investigations of Laser Damage to Ocular Tissues," Final Report, Contract AF 33615-67-C-1752, SRI Project 6680, Stanford Research Institute, Menlo Park, California (March 1968).

3. A. Vassiliadis, R. C. Rosan, and H. C. Zweng, "Research on Ocular Laser Thresholds," Final Report, Contract F41609-68-C-004, SRI Project 7191, Stanford Research Institute, Menlo Park, California (August 1969).

4. Lt. Col. P. W. Lappin, Paper presented at Second International Laser Safety Conference, Cincinnati, Ohio (24-25 March 1969).

5. T. H. Wood, "Lethal Effects of High and Low Temperatures on Unicellular Organisms," Advances in Biological and Medical Physics, Vol. IV (Academic Press, New York, New York, 1956).

6. J. J. Vos, "A Theory of Retinal Burns," Bull. Math. Phys., Vol. 24, p. 115 (1962).

7. W. T. Ham et al., "Flashburns in Rabbit Retina," Am. J. Ophth., Vol. 46, p. 700 (1958).

8. W. T. Ham et al., Trans. N.Y. Acad. Sci., Vol. 28, p. 517 (1966).

9. A. M. Clarke, W. J. Geeraets, and W. T. Ham, Appl. Optics, Vol. 8, p. 1051 (1969).

10. W. P. Hansen, L. Feigen, and S. Fine, Appl. Optics, Vol. 6, p. 1973 (1967).

11. S. Glasstone, K. J. Laidler, and J. Eyring, The Theory of Rate Processes (McGraw Hill Book Co., Inc., New York, 1941).

12. F. H. Johnson, H. Eyring, and M. J. Polissar, "The Kinetic Basis of Molecular Biology" (John Wiley & Sons, New York, 1954).

13. A. Vassiliadis, "Ocular Damage from Laser Radiation," in Laser Applications in Medicine and Biology, M. L. Wolbarsht, Ed. (Plenum Press, New York, 1971).